35）厚生労働省医薬食品局食品安全部長, 食安第 1228 第 7 号 (2012).
通知は以下のアドレスから閲覧できる
http://www.mhlw.go.jp/topics/bukyoku/iyaku/syoku-anzen/gyousei/dl/121228_2.pdf

Biochimie 95 (2013) 309–319

Contents lists available at SciVerse ScienceDirect

Biochimie

journal homepage: www.elsevier.com/locate/biochi

Research paper

Biochemical and functional characterization of novel NADH kinase in the enteric protozoan parasite *Entamoeba histolytica*☆

Ghulam Jeelani [a,b], Afzal Husain [a,c,1], Dan Sato [d], Tomoyoshi Soga [d], Makoto Suematsu [b], Tomoyoshi Nozaki [a,e,*]

[a] *Department of Parasitology, National Institute of Infectious Diseases, 1-23-1 Toyama, Shinjuku, Tokyo 162-8640, Japan*
[b] *Department of Biochemistry and Integrative Medical Biology, School of Medicine, Keio University, Shinjuku, Tokyo 160-8582, Japan*
[c] *Department of Parasitology, Graduate School of Medicine, Gunma University, Maebashi 371-8511, Japan*
[d] *Institute for Advanced Biosciences, Keio University, Tsuruoka, Yamagata 997-0052, Japan*
[e] *Graduate School of Life and Environmental Sciences, University of Tsukuba, 1-1-1 Tennodai, Tsukuba, Ibaraki 305-8572, Japan*

ARTICLE INFO

Article history:
Received 16 April 2012
Accepted 27 September 2012
Available online 13 October 2012

Keywords:
Entamoeba histolytica
NADH kinase
Oxidative stress
Nicotinamide (pyridine) nucleotide
Reactive oxygen species

ABSTRACT

NAD(H) kinase catalyzes the phosphorylation of NAD(H) to form NADP(H) using ATP or inorganic polyphosphate as a phosphoryl donor. While the enzyme is conserved throughout prokaryotes and eukaryotes, remarkable differences in kinetic parameters including substrate preference, cation dependence, and physiological roles exist among the organisms. In the present study, we biochemically characterized NAD(H) kinase from the anaerobic/microaerophilic fermentative protozoan parasite *Entamoeba histolytica*, which lacks the conventional mitochondria capable of oxidative phosphorylation, leading to ATP. The kinetic properties of *E. histolytica* NAD(H) kinase recombinantly produced in *Escherichia coli* showed remarkable differences from those in bacteria and higher eukaryotes. *Entamoeba* NAD(H) kinase preferred NADH to NAD+ as the phosphoryl acceptor, utilized nucleoside triphosphates including ATP, GTP and deoxyATP, but not nucleoside di-, mono-phosphates, or inorganic polyphosphates, as the phosphoryl donor. To further understand the physiological roles in *E. histolytica*, we generated a stable transformant overexpressing NAD(H) kinase. Overexpression of NAD(H) kinase resulted in a 1.6–2 fold increase in the NADPH and NADP+ concentrations, a 40% reduction of the intracellular concentration of reactive oxygen species, and also led to increased tolerance toward hydrogen peroxide. These data, together with the essentially of NAD(H) kinase gene, underscore its significance as an NADP(H)-producing enzyme in this organism, and should help in designing of drugs targeting this enzyme.

1. Introduction

Entamoeba histolytica is one of the most widespread and clinically important parasites, causing both serious intestinal (amoebic colitis) and extraintestinal (amoebic liver abscess) diseases throughout the world [1]. World Health Organization (WHO) claimed that *E. histolytica* is placed second only after *Plasmodium falciparum* as a parasitic protozoan pathogen responsible for 70,000 annual deaths [2]. Metronidazole and related 5-nitroimidazole compounds are commonly used against invasive intestinal and extraintestinal amebiasis, while there are not other available alternative drugs effective against amebiasis [3]. Although clinical resistance against metronidazole has not yet been demonstrated, sporadic cases of treatment failure have been reported [3]. In addition, it has been shown that this parasite easily adapts to therapeutic levels of metronidazole in vitro [4], (Penuliar et al., unpublished). Therefore, the development of new antiamebic drug(s), and the identification and characterization of metabolic pathways and enzymes which are unique to *E. histolytica* and essential for its survival and proliferation is urgently required. One of such enzymes which we characterized in the present study is NAD(H) kinase.

Abbreviations: EhNadhk, *Entamoeba histolytica* NAD(H) kinase; INT, iodonitrotetrazolium; 2′,7′-DCF-DA, 2′,7′-dichlorodihydrofluorescein; ROS, reactive oxygen species.

☆ The nucleotide sequence data of *E. histolytica* NADH kinase reported in this paper is available at the DDBJ/GenBank®/EBI data bank with the accession number JQ036180.

* Corresponding author. Department of Parasitology, National Institute of Infectious Diseases, 1-23-1 Toyama, Shinjuku-ku, Tokyo 162-8640, Japan. Tel.: +81 3 4582 2690; fax: +81 27 5285 1219.
E-mail address: nozaki@nih.go.jp (T. Nozaki).
[1] Present address: Department of Immunology and Genomic Medicine, Kyoto University Graduate School of Medicine, Yoshida, Sakyo-ku, Kyoto 606-8501, Japan.

0300-9084/$ – see front matter © 2012 Elsevier Masson SAS. All rights reserved.
http://dx.doi.org/10.1016/j.biochi.2012.09.034

NAD(H) kinase (E.C. 2.7.1.86) is a key enzyme that regulates the NAD(H)/NADP(H) concentrations in the cell. It is the only enzyme responsible for the de novo NADP+/NADPH synthesis from NAD+/NADH [5]. NAD(H) kinase can be ubiquitously found in most, if not all, of the sequenced genome of living organisms, including prokaryotes and eukaryotes. In most organisms, there is only one NAD(H) kinase, whereas, in some organisms, two to three NAD(H) kinase isozymes exist. For example, two NAD(H) kinases, NadF and NadG, were found in *Salmonella typhimurium* [6]; two NAD(H) kinases isozymes with distinct substrate specificities toward nucleotide triphosphates and K_m values are present in *Euglena gracilis* [7]. There are three functionally non-interchangeable NAD(H) kinases in *Saccharomyces cerevisiae*; Pos5p exists in the mitochondrial matrix, while Utr1p and Yef1p exist in the cytoplasm [8–10]. It has also been shown that mitochondrial NAD(H) kinase from *S. cerevisiae* is required for iron sulfur cluster biogenesis [11]. NAD(H) kinase has been demonstrated to be essential in many organisms, including *Mycobacterium tuberculosis* [12], *Bacillus subtilis* [13], *Escherichia coli* [14], and *Salmonella enterica* [15], where NAD(H) kinase is encoded by a single gene. Humans also possess a single NAD(H) kinase gene, which was well characterized [16]. It has been reported that bacterial NAD(H) kinase shows significant functional diversity from its human counterpart, and it can be regarded as an attractive target for the development of antibacterial drugs [17].

In contrast to bacteria and higher eukaryotes, a scenario of NADP(H) biosynthesis and the physiological role of their direct production from NAD(H) in protozoan parasites remain largely unknown. In this study, we characterized for the first time the kinetic properties and potential roles of NAD(H) kinase in *E. histolytica*. We demonstrated that NAD(H) kinase is involved in maintenance of the cellular NADP+ pool and also plays an important role in response to oxidative stress.

2. Materials and methods

2.1. Chemicals and reagents

NAD+, NADP+, and trans-epoxysuccinyl-L-leucylamido-(4-guanidino) butane, ATP were purchased from Sigma–Aldrich (Tokyo, Japan). Ni^{2+}-NTA agarose was purchased from Novagen (Darmstadt, Germany). Lipofectamine and geneticin (G418) were purchased from Invitrogen (Carlsbad, CA, USA). All other chemicals of analytical grade were purchased from Wako (Tokyo, Japan) unless otherwise stated.

2.2. Microorganisms and cultivation

Trophozoites of the *E. histolytica* clonal strain HM1: IMSS cl 6 and G3 strain [18], kindly provided by David Mirelman, Weisman Institute, Israel, were maintained axenically in Diamond's BI-S-33 medium at 35.5 °C as described previously [19]. Trophozoites were harvested in the late-logarithmic growth phase for 2–3 days after inoculation of one-thirtieth to one-twelfth of the total culture volume. After the cultures were chilled on ice for 5 min, trophozoites were collected by centrifugation at 500 × *g* for 10 min at 4 °C and washed twice with ice-cold PBS, pH 7.4. *E. coli* BL21 (DE3) strain was purchased from Invitrogen.

2.3. Amino acid comparison and phylogenetic analysis

Amino acid sequences of NAD(H) kinase or putative NAD(H) kinase-like proteins were obtained from 40 other organisms deposited in DDBJ/EBI/GenBank database by using blastp search with *E. histolytica* NAD(H) kinase, described in this paper, as a query. Multiple sequence alignment of these proteins was generated using CLUSTAL W program [20]. The alignment obtained by CLUSTAL W was inspected and manually corrected using Genedoc program (www.psc.edu/biomed/genedoc) [21]. After all gaps were removed, 326 unambiguously-aligned residues were selected for phylogenetic analyses. The neighbor-joining and maximum parsimony methods were performed using MEGA4.1 program [22]. A final phylogenetic tree of 30 sequences was drawn by MEGA4.1. The branch lengths and bootstrap values of 1000 replicates (in percentage) in these trees were obtained from the neighbor-joining analysis.

2.4. Construction of a plasmid for the production of recombinant *E. histolytica* NAD(H) kinase

Standard techniques were used for cloning and plasmid construction as previously described [23]. A fragment was cloned to produce a fusion protein containing a histidine-tag (provided by the vector) at the amino terminus. A DNA fragment corresponding to cDNA encoding *E. histolytica* NAD(H) kinase (designated here in after as EhNadhk) was amplified by PCR using the *E. histolytica* cDNA library [24] as a template and oligonucleotide primers. The sense and antisense oligonucleotide primers used for EhNadhk were: 5′-GAA**GGATCC**ATGACTACTCTTCAGATTGA-3′ and 5′-GAA**GT CGAC**TTATTCAAAGAAATCCTTAG-3′ where bold letters indicate *Bam*HI and *Sal*I restriction sites. PCR was performed with platinum *pfx* DNA polymerase (Invitrogen) and the following parameters: an initial incubation at 94 °C for 2 min; followed by the 30 cycles of denaturation at 94 °C for 15 s; annealing at 50, 45, or 55 °C for EhNadhk, respectively, for 30 s; and elongation at 68 °C for 2 min; and a final extension at 68 °C for 10 min. The PCR fragment was digested with *Bam*HI and *Sal*I, electrophoresed, purified with Gene clean kit II (BIO 101, Vista, CA, USA), and ligated into *Bam*HI and *Sal*I digested pCOLD-1 (Novagen) in the same orientation as the T7 promoter to produce pCOLD1-EhNadhk. The nucleotide sequence of the cloned EhNadhk was verified by sequencing to be identical to the putative protein coding region of AFD32557 (accession number, XP_657388).

2.5. Bacterial expression and purification of recombinant *E. histolytica* NAD(H) kinase (rEhNadhk)

The above mentioned plasmid was introduced into *E. coli* BL21 (DE3) cells by heat shock at 42 °C for 1 min. *E. coli* BL21 (DE3) harboring pCOLD1-EhNadhK was grown at 37 °C in 100 ml of Luria Bertani medium in the presence of 50 μg/ml ampicillin. The overnight culture was used to inoculate 500 ml of fresh medium, and the culture was further continued at 37 °C with shaking at 180 rpm. When A_{600} reached 0.6, 1 mM of isopropyl β-D-thio galactopyranoside was added, and cultivation was continued for another 24 h at 15 °C. *E. coli* cells from the induced culture were harvested by centrifugation at 4050 × *g* for 20 min at 4 °C. The cell pellet was washed with PBS, pH 7.4, re-suspended in 20 ml of the lysis buffer (50 mM Tris–HCl, pH 8.0, 300 mM NaCl, and 10 mM imidazole) containing 0.1% Triton ×100 (v/v), 100 μg/ml lysozyme, and 1 mM phenylmethyl sulfonyl fluoride, and incubated at room temperature for 30 min, sonicated on ice and centrifuged at 25,000 × *g* for 15 min at 4 °C. The supernatant was mixed with 1.2 ml of 50% Ni^{2+}-NTA His-bind slurry, incubated for 1 h at 4 °C with mild shaking. The recombinant EhNadhk-bound resin in a column was washed three times with buffer A [50 mM Tris–HCl, pH 8.0, 300 mM NaCl, and 0.1% Triton X-100, v/v] containing 10–50 mM of imidazole. Bound proteins were eluted with buffer A containing 100–300 mM imidazole. After the integrity and the purity of rEhNadhk protein were confirmed with 12% SDS-PAGE analysis, followed by

Coomassie Brilliant Blue staining, they were extensively dialyzed twice against the 300-fold volume of 50 mM Tris–HCl, 150 mM NaCl, pH 8.0 containing 10% glycerol (v/v) and the Complete Mini protease inhibitor cocktail (Roche, Mannheim, Germany) for 18 h at 4 °C. The dialyzed proteins were stored at −80 °C with 20% glycerol in small aliquots until further use. Protein concentrations were spectrophotometrically determined by the Bradford method using bovine serum albumin as a standard as previously described [25].

2.6. Enzyme assays

The ATP-dependent NAD kinase activity was assayed at 37 °C by the modified method described previously [26], unless otherwise stated. Briefly, the formation of NADP(H) was continuously measured at $A340$ (ε = 6.67 mM^{-1} cm^{-1}) in a reaction mixture comprising 10 mM NAD+, 5.0 mM ATP, 5 mM $MgCl_2$, 5.0 mM glucose-6-phosphate,0.5 U glucose-6-phosphate dehydrogenase, 100 mM Tris–HCl (pH 7.5), and an appropriate amount of rEhNadhk.

The ATP-dependent NADH kinase activity was monitored in a coupling assay, in which INT reduction at 490 nm was monitored in a reaction mixture comprising 2 mM NADH, 5.0 mM ATP, 5 mM $MgCl_2$, 100 mM Tris–HCl (pH 7.5), 0.5 mM INT, and an appropriate amount of rEhNadhk and rEhNO1 [27]. In order to determine the activity, linearity was confirmed using at least two concentrations of the enzyme preparations at more than two time points. The kinetic parameters were estimated using the non-linear regression function obtained from the GraphPad Prism software (GraphPad Software Inc., San Diego, CA). These kinetic values are presented as the means ± S.E. for three independent determinations and are reproducible within ±10% S.E. of the mean value. One unit of enzyme activity was defined as 1.0 μmol of NADP+ or NADPH produced in 1 min at 37 °C. The experiments were repeated in triplicate with proteins isolated from two independent extractions.

2.7. Production of E. histolytica transformants overexpressing EhNadhK

The protein coding region of EhNadhk was amplified by PCR from cDNA using sense and antisense oligonucleotides containing appropriate restriction sites at the 5′ end. The sense and antisense oligonucleotide primers used for EhNadhk were: 5′-CTA**CCCGG-G**ATGACTACTCTTCAGATTGAT-3′ and 5′-CAA**CTCGAG**TTATTCAAA-GAAATCCTTAGT-3′ (restriction sites are shown in bold). The PCR-amplified DNA fragment was digested with *Sma*I and *Xho*I, and ligated into *Sma*I and *Xho*I sites of the expression vector pEhExHA [28] to produce pEhExHA-Nadhk. Plasmids were introduced into the amoeba trophozoites by liposome-mediated transfection as previously described [29]. Transformants were initially selected in the presence of 3 μg/ml of geneticin. The geneticin concentration was gradually increased to 6–20 μg/ml during next 2 weeks before the transformants were subjected to analyses.

2.8. Production of EhNadhk gene-silenced strain

In order to construct a plasmid for epigenetic silencing [18,30] of EhNadhk, a fragment corresponding to a 420-bp long 5′ end of open reading frame of *EhNadhk* gene was amplified by PCR from cDNA using sense 5′-TAT**AGGCC**TATGACTACTCTTCAGATTGAT-3′ and antisense 5′-CAG**GAGCTC**TCCATTAATAATAACTTCAAA-3′ oligonucleotides containing StuI and SacI restriction sites (restriction sites are shown in bold). The PCR amplified products were digested with *Stu*I and *Sac*I, and ligated into the *Stu*I- and *Sac*I-double digested psAP2-Gunma [31] to construct gene silencing plasmids psAP2G-Nadhk. The trophozoites of G3 strain were transformed with either empty vector or silencing plasmid by liposome-mediated transfection as previously described [29]. Transformants were initially selected in the presence of 1 μg/ml geneticin, and the geneticin concentrations were gradually increased during next two weeks prior to subjecting the transformants to analyses.

2.9. Assay of hydrogen peroxide sensitivity

To examine sensitivity to H_2O_2, *E. histolytica* transformants possessing pEhExHA-Nadhk and pEhExHA were seeded into wells on a 96-well plate (10^4 trophozoites per well) in BI-S-33 medium containing 20 μg/ml geneticin and incubated for 4–6 h at 35.5 °C. The cells were then exposed to varying concentrations (0.2–6.4 mM) of H_2O_2 for 12 h in the same culture medium. Following incubation, medium was removed and 100 μL pre-warmed Opti-MEM® I (Invitrogen) containing 10% (v/v) Cell Proliferation Reagent WST-1 (Roche Diagnostics, Mannheim, Germany) was added. After 1 h of incubation at 35.5 °C, the optical density at A450 was measured with that at A595 as a reference using a microplate reader (Model 550, Bio-Rad, Tokyo, Japan). The initial density and incubation period of the cultures were chosen to maintain the control trophozoites in the late-logarithmic growth phase throughout the experiment, and also to allow the measurement of optical density in the linear portion of the curves. The assays were performed three times in triplicate.

2.10. Quantitation of reactive oxygen species

Fluorescence spectrophotometry was used to measure the production of intracellular reactive oxygen species using 2′,7′-DCF-DA as a probe as previously described [32]. Briefly, *E. histolytica* transformants containing pEhExHA-Nadhk or pEhExHA were cultivated in BI-S-33 medium with or without 0.8 mM H_2O_2 for 12 h. After cells were washed with PBS and 5.0×10^5 cells were incubated in 1 ml of PBS containing 20 μM 2′,7′-DCF-DA for 30 min at 35.5 °C in the dark. The intensity of fluorescence was immediately read at excitation and emission wavelengths of 492 and 519 nm, respectively.

2.11. Measurement of pyridine nucleotides

The concentrations of NAD+, NADH, NADP+, and NADPH were chemically determined with NAD+/NADH and NADP+/NADPH quantification kits (Biovision) according to the manufacturer's instructions.

2.12. Measurement of purine and pyrimidine nucleotide concentrations

Nucleotides concentrations were determined by using CE-TOFMS as described previously [33]. Approximately $1{,}5 \times 10^6$ cells were harvested and washed twice with 5% mannitol. The cells were immediately suspended in 1.6 ml of −75 °C methanol to quench metabolic activity. To ensure that experimental artifacts such as ion suppression did not lead to misinterpretation of metabolite levels, internal standards, 2-(*N*-morpholino) ethanesulfonic acid, methionine sulfone, and D-camphor-10-sulfonic acid were added to each sample. The samples were then sonicated for 30 s and then mixed with 1.6 ml of chloroform and 640 μl of deionized water. After vortexing, the mixture was centrifuged at 4600 × *g* at 4 °C for 5 min. The aqueous layer (1.6 ml) was filtrated using an Amicon Ultrafree-MC ultrafilter (Millipore Co., Massachusetts, USA) and centrifuged at 9100 × *g* at 4 °C for approximately 2 h. The filtrate was dried and preserved at −80 °C until mass spectrometric analysis [34]. Prior to the analysis, the sample was dissolved in 20 μl of deionized water containing reference compounds (200 μmol/L each of 3-aminopyrrolidine and trimesic acid). CE-TOFMS was performed using an Agilent CE Capillary Electrophoresis System equipped with an Agilent 6210 Time-of-Flight mass spectrometer, Agilent 1100 isocratic HPLC pump, Agilent G1603A CE-MS adapter kit,

and Agilent G1607A CE-ESI-MS sprayer kit (Agilent Technologies, Waldbronn, Germany). The system was controlled by Agilent G2201AA ChemStation software for CE. Data acquisition was performed by Analyst QS software for Agilent TOF (Applied Biosystems, CA, USA; MDS Sciex, Ontario, Canada).

2.13. Immunoblot analysis

Cell lysates and culture supernatants were separated on 12% (w/v) SDS-polyacrylamide gel electrophoresis and subsequently electrotransferred onto nitrocellulose membranes (Hybond-C Extra; Amersham Biosciences UK, Little Chalfont, Bucks, UK) as described [35]. Non-specific binding was blocked by incubating the membranes for 1.5 h at room temperature in 5% non-fat dried milk in TBST (50 mM Tris–HCl, pH 8.0, 150 mM NaCl and 0.05% Tween-20). The blots were reacted with primary antibodies specific for EhNadhk, HA and cysteine synthase 1 [24] as a control for membrane and cytosolic fraction, respectively, at a dilution of 1:500 to 1:100. Antisera were raised against purified recombinant EhNadhk in rabbits commercially (Operon, Tokyo, Japan). The membranes were washed with TBST and further reacted with alkaline phosphatase-conjugated anti-rabbit (1:2000) for 1 h. After further washings with TBST, specific proteins were visualized with an alkaline phosphatase conjugate substrate kit (Bio-Rad) and scanned with Image Scanner (Amersham Pharmacia Biotech, Piscataway, NJ, USA).

3. Results

3.1. Identification of NAD(H) kinase (Nadhk) gene and its encoded protein from E. histolytica

We identified a gene encoding Nadhk by homology search against the *E. histolytica* genome database (http://amoebadb.org/amoeba/) using bacterial Nadhk sequences. We designated this gene as *EhNadhk* (corresponding to EHI_151920 and XP_657388). *EhNadhk* gene contains a 786 bp open reading frame, which encodes the protein of 262 amino acid residues with a predicted molecular mass of 29.5 and p*I* of 6.5, respectively.

3.2. Features of the deduced protein sequence of EhNadhk

Database search and multiple sequence alignment of representative NAD(H) kinases from different lineages with that of *E. histolytica* Nadhk showed 20% sequence identity to the polyphosphate/ATP-dependent NAD kinase from *M. tuberculosis* [36], 15% and 18% identity to the ATP-dependent NAD kinase from *E. coli* and human [37,16], respectively. EhNadhk shows the highest amino acid identity to NAD kinase from *Trypanosoma brucei* (XP_846131) and *Leishmania major* (XP_001680816) (88% and 85%, respectively). All motifs shown to be conserved among NAD kinase, including the conserved domain I, NE/D motif, and conserved region II, are well conserved in EhNadhk (Fig. 1).

3.3. Phylogenetic analysis

Phylogenetic reconstruction was performed by the neighbor joining and maximum parsimony programs using 30 NAD(H) kinase sequences from representative organisms. NAD(H) kinases from *Entamoeba, Trypanosoma*, and *Leishmania* show monophyly and are distinguishable from other NAD(H) kinases, including *E. coli* and human NAD(H) kinase (Fig. 2). It was also suggested that *E. histolytica* and kinetoplastids obtained this gene by lateral gene transfer from proteobacteria, similar to a number of metabolic enzymes [38]. Phylogenetic reconstruction using the maximum parsimony method also supports the above-mentioned conclusion (data not shown).

3.4. Expression and purification of recombinant EhNadhk

The recombinant EhNadhk was overproduced at the level of 2.0–2.5% of the total soluble proteins in *E. coli* BL21 cells. SDS-PAGE analysis followed by Coomassie Brilliant Blue staining showed that the purified rEhNadhk protein was present as a single 32-kDa homogenous protein, under reducing conditions (Fig. 3). The mobility of rEhNadhk was consistent with the predicted size of the monomeric EhNadhk proteins with an extra 2.6 kDa histidine tag added at the amino terminus. The purity of rEhNadhk was estimated more than 95% as judged by densitometric scanning of the stained gel. rEhNadhk protein was stable and retained its full activity when stored with 10–15% glycerol at −30 or −80 °C for at least 3 months.

3.5. Acceptor preference and kinetics properties of rEhNadhk

EhNadhk utilized both NADH and NAD+, with a higher preference for NADH (Table 1). The pH activity profile of EhNadhk displayed a broad and symmetrical profile with maximal activity at pH 7.5 (data not shown). No difference in the pH activity profile was observed between NAD+ and NADH used as a phosphate acceptor. Therefore, all kinetic studies were performed at pH 7.5. Table 1 summarizes the apparent K_m, V_{max}, and k_{cat} values for NAD+ and NADH. Both diphospho nicotinamide nucleotides exhibited hyperbolic saturation kinetics when assayed over the ranges 0.1–12 mM and 0.01–4 mM for NAD+ and NADH, respectively (data not shown). The K_m and k_{cat}/K_m values of rEhNadhk toward NAD+ and NADH were largely different. The catalytic efficiency (k_{cat}/K_m) for NADH was approximately 40-fold higher than that obtained with NAD+, and therefore, the protein was designated as *E. histolytica* NADH kinase (EhNadhk). The enzyme showed maximum activity with 4–5 mM ATP. When the ATP concentration was increased to more than 6 mM, NADH kinase activity was inhibited; approximately 50% inhibition was observed at 10 mM ATP. Although we also examined whether this enzyme catalyzes a reverse reaction, no activity was detected in the reverse direction using either NADP+ or NADPH as a substrate.

3.6. Phosphoryl donor specificities of EhNadhk

Recombinant NADH kinase used several nucleoside triphosphates, such as ATP, CTP, GTP, and UTP, as phosphoryl donors (Table 2). However, neither nucleoside monophosphates nor poly(P)s (pyrophosphate, tripolyphosphate, trimetaphosphate, hexametaphosphate, metaphosphate, and polyphosphate) served as a phosphoryl donor. Glucose 6-phosphate and phosphoenolpyruvate were also inert as phosphoryl donors. ATP, GTP and dATP were utilized more effectively than other nucleoside triphosphates. The enzyme also utilized nucleoside diphosphate (ADP) as a phosphoryl donor to a lesser extent than nucleoside triphosphate.

3.7. Effects of metal ions on EhNadh kinase activity

The effect of metal ions was examined by assaying the activity after the addition of metal salts to the standard reaction mixture. EhNadhk showed an absolute requirement for a free bivalent metal cofactors, with Mg^{2+} as the preferred cation (Table 3). However, no activity was detected in presence of monovalent metal ions (Li^+, Na^+, and K^+).

3.8. Nadhk activity controls the cellular concentrations of NADP+ in E. histolytica

We next investigated the role of Nadhk on the cellular pyridine nucleotide concentrations in. *E. histolytica* by creating stable transformants that overexpressed HA-tagged EhNadhk. HA-tagged

```
E. histolytica    ------------------------------------------------------------ 1
H. sapiens        MEMEQEKMTMNKELSPDAAAYCCSACHGDETWSYNHPIRGRAKSRSLSASPALGSTKEFR 60
E. coli           ------------------------------------------------------------ 1
M. tuberculosis   ------------------------------------------------------------ 1

E. histolytica    -------------------------------------------MTTLQIDHIRAKFHID 16
H. sapiens        RTRSLHGPCPVTTFGPKACVLQNPQTIMHIQDPASQRLTWNKSPKSVLVIKKMRDASLLQ 120
E. coli           ----------------------------------MNNHFKCIGIVGHPRHPTALT 21
M. tuberculosis   ----------------------------------MTAHRSVLLVVHTGRDEATET 21

E. histolytica    DYNQKAPDVARQFERIHDEVNPN-------------------------------VVMT 43
H. sapiens        PFKELCTHLMEENMIVYVEKKVLEDPAIASDESFGAVKKKFCTFREDYDDISNQIDFIIC 180
E. coli           THEMLYRWLCTKGYEVIVEQQIAHELQLKNVKTG------------TLAEIGQLADLAVV 69
M. tuberculosis   ARRVEKVLGDNKIALRVLSAEAVDRGSLHLAPDDMRAMGVEIEVVDADQHAADGCELVLV 81

                  Conserved domain I
E. histolytica    FGGDGTFLKAFHENYHLQLPYLGINCGNVGYLINPIQEVMDSIEQNKPLKCYSYP---CL 100
H. sapiens        LGGDGTLLYASSLFQGSVPPVMAFHLGSLGFLTPFSFENFQSQVTQVIEGNAAVVLRSRL 240
E. coli           VGGDGNMLGAARTLARYDIKVIGINRGNLGFLTDLDPDNAQQQLADVLEGHYISEKRFLL 129
M. tuberculosis   LGGDGTFLRAAELARNASIPVLGVNLGRIGFLAEAEAEAIDAVLEHVVAQDYRVEDRLTL 141
                   ****  *
                                                          NE/D motif
E. histolytica    KVDASNGSTQLSTQLA-------------------------FNDAWIER-LNGQCCWFE 133
H. sapiens        KVRVVKELRGKKTAVHNGLGENGSQAAGLDMDVGKQAMQYQVLNEVVIDRGPSSYLSNVD 300
E. coli           EAQVCQQDCQKRISTA-------------------------INEVVLHPGKVAHMIEFE 163
M. tuberculosis   DVVVRQGGRIVNRGWA-------------------------LNEVSLEKGPRLGVLGVV 175
                                                           *
                                  Conserved domain II
E. histolytica    VIINGVVRIPKLCCDGIVVCTPAGSTGYSKSIGVMPIPPNANMIGFVPNNASYPLGIRPL 193
H. sapiens        VYLDGHL-ITTVQGDGVIVSTPTGSTAYAAAAGASMIHPNVPAIMITP-ICPHSLSFRPI 358
E. coli           VYIDEIF-AFSQRSDGLIISTPTGSTAYSLSAGGPILTPSLDAITLVP-MFPHTLSARPL 221
M. tuberculosis   VEIDGRP-VSAFGCDGVLVSTPTGSTAYAFSAGGPVLWPDLEAILVVP-NNAHALFGRPM 233
                             # **    ** *** *    *     *

E. histolytica    YLPLDTEVIVKNIQPNRRKTRGFYDGVELNEITELKIKAIENGCR-VIYAHEENLNKTYI 252
H. sapiens        VVPAGVELKIMLSPEARNTAWVSFDGRKRQEIRHGDSISITTSCYPLPSICVRDPVSDWF 418
E. coli           VINSSSTIRLRFS-HRRNDLEISCDSQIALPIQEGEDVLIRRCDYHLNLIHPKD--YSYF 278
M. tuberculosis   VTSPEATIAIEIEADGHD-ALVFCDGRREMLIPAGSRLEVTRCVTSVKWARLDS--APFT 290

E. histolytica    NKVTKDFFE---------- 261
H. sapiens        ESLAQCLHWNVRKKQAHFEEEEEEEEEG 446
E. coli           NTLSTKLGWSKKLF------------- 292
M. tuberculosis   DRLVRKFRLPVTGWRGK---------- 307
```

Fig. 1. Alignment of the NAD(H) kinase protein sequences from *E. histolytica* and other organisms. The sequences were aligned using the CLUSTAL W program. The three highly conserved domains, XGGDGXXL (conserved domain I), NE/D, and DGXXXXTPXGSTXY (conserved domain II) are boxed. Identical residues in these conserved domains are denoted by asterisks (*). The species name abbreviations and the NCBI accession numbers of the NAD kinase genes are as follows: *E. histolytica* (XP_657388); *H. sapiens*, *Homo sapiens* (CAA20354); *E. coli*, *Escherichia coli* (NP_417105); *M. tuberculosis*, *Mycobacterium tuberculosis* (BAB21478). The residue important for NAD or NADH preference previously described (41), is indicated by a sharp (#) with gray background.

EhNadhk-expressing transformant expressed approximately 2.4 fold higher level of the corresponding enzyme compared to control transformant (Fig. 4A). In HA-tagged EhNadhk-expressing transformant, the NADP+ and NADPH concentrations were increased by 2.1 ± 0.4 (mean ± standard deviation) and 1.6 ± 0.2 fold, respectively, whereas the concentration of NAD+ was decreased by 61 ± 11%, and NADH concentration remained unchanged (Fig. 5B). We also examined the levels of the nucleoside triphosphates in stable transformants that overexpressed HA-tagged EhNadhk. ATP and GTP concentrations were significantly decreased in the HA-tagged EhNadhk-expressing transformant (25 and 22%, respectively), suggesting that ATP and GTP might be utilized to synthesize NADP+/NADPH from NAD+/NADH. Alternatively, the decrease in ATP and GTP levels may be due to the higher increase of energy requirement to synthesize the overexpressed enzyme(s). There was also a slight decrease in the level of ADP and GDP. In contrast, the levels of nucleoside monophosphates (AMP, GMP, and CMP) remained unchanged (Fig. 4B).

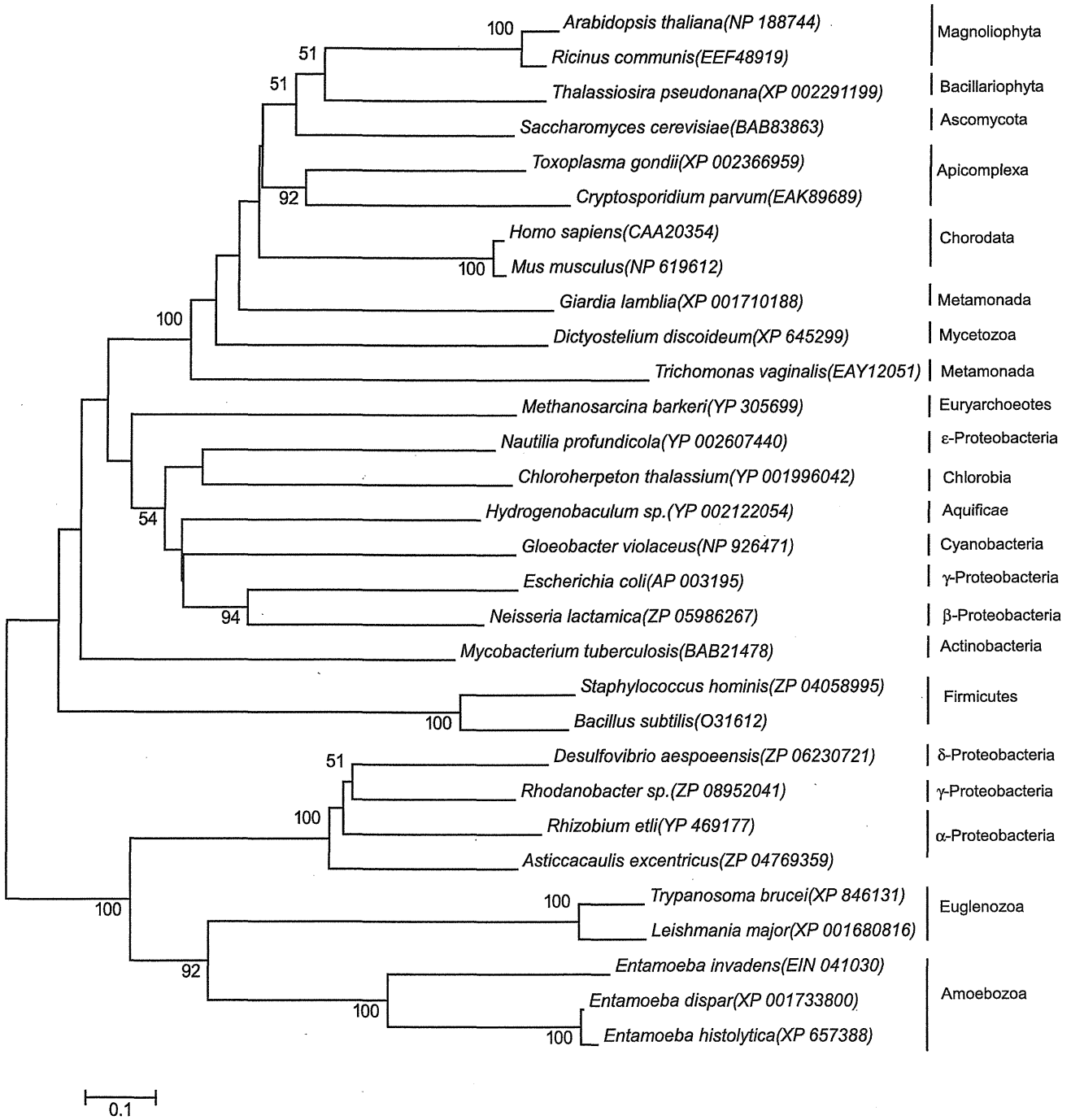

Fig. 2. Phylogenetic reconstructions of NAD(H) kinase proteins from *E. histolytica* and other organisms. Phylogenetic trees of 30 NAD kinase sequences were constructed using the CLUSTAL W program and drawn with the MEGA4.1 program, and a representative neighbor-joining tree is shown. The numbers at the nodes represent the bootstrap values as a percentage of 1000 replicates. The scale bar indicates 0.1 substitutions at each amino acid position. Species names and accession numbers of the sequences are also indicated.

3.9. NADH kinase overexpression leads to increased tolerance to oxidative stress

We investigated whether overexpression of Nadhk affects sensitivity against oxidative stress. The stable transformant that overexpressed EhNadhk and control transformant were exposed to different concentrations of H_2O_2 (0–6.4 mM) for 12 h, and viability was determined. The EhNadhk overexpressing transformant showed partial resistance against 0.8–3.2 mM H_2O_2 compared to control transformant, suggesting that Nadhk overexpression protected the cells against oxidative stress (Fig. 5A). We also quantitated the levels of nicotinamide nucleotides in the EhNadhk-overexpressing and control (pEhExHA) transformants that were incubated under normal conditions or exposed to 0.8 mM H_2O_2 for 12 h (Fig. 5B). When compared to untreated control, the level of NAD+ and NADH was decreased by 40% upon H_2O_2 treatment in the

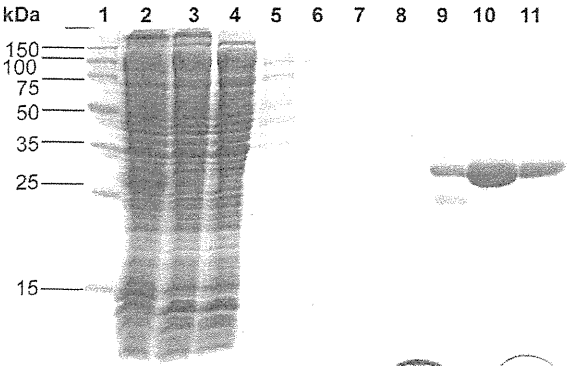

Fig. 3. Expression and purification of recombinant EhNadhk. Protein samples at each step of purification were subjected to 15% SDS-PAGE under reducing conditions, and then stained with Coomassie Brilliant Blue R250. Lane 1, molecular weight markers; lane 2, the total lysate; lane 3, supernatant fraction; lane 4, unbound fraction; lanes 5–9, fractions eluted with 10, 20, 30, 50, and 100 mM imidazole, respectively; lanes 10–11, purified recombinant EhNadhk, eluted with 200 and 300 mM imidazole, respectively.

control transformant, whereas the level of NADPH and NADP+ was increased 1.3 or 2.0 fold, respectively. However, when control and EhNadhk-overexpressing transformants were compared under oxidative stress conditions (hatched versus black bars), no statistically significant difference was found in the levels of NAD+, NADP+, and NADH, whereas there was significant increase (1.5 fold) in the level of NADPH (Fig. 5B). The increased NADPH is likely attributable to the higher content of NADP+ available to be reduced, which may be produced by other reaction(s). The increased NADPH appears to account for the increased resistance to H_2O_2 treatment of the EhNadhk-overexpressing transformant (Fig. 5A).

3.10. Nadhk overexpression represses the production of intracellular ROS upon H_2O_2 exposure

Since NADPH generally plays an indispensable role in oxidative defense mechanisms, it was of interest to examine the effect of augmented Nadhk expression on the amount of intracellular ROS. The relative level of ROS in the Nadhk-overexpressing transformant under normal and oxidative stress conditions was measured using the fluorescent indicator CM-H_2DCFDA. The endogenous ROS level under a non-stress condition in Nadhk-overproducing strain was 40% lower compared to that in control strain (Fig. 5C). When challenged with 0.8 mM H_2O_2, the amount of ROS detected in the Nadhk-overexpressing cells was reduced by 43% compared to that in control (Fig. 5C).

Table 1
Kinetic parameters of NADH kinase.

A. NAD kinase reaction				
Substrate	K_m (mM)	V_{max} (μmole/min/mg)	k_{cat} (min^{-1})	k_{cat}/K_m (min^{-1} mM^{-1})
ATP	1.74 ± 0.12	3.79 ± 0.11	121 ± 3	69.8 ± 29.3
NAD^+	1.59 ± 0.18	3.56 ± 0.12	114 ± 4	71.7 ± 19.9
B. NADH kinase reaction				
Substrate	K_m (mM)	V_{max} (μmole/min/mg)	k_{cat} (min^{-1})	k_{cat}/K_m (min^{-1} mM^{-1})
ATP	0.40 ± 0.02	5.01 ± 0.08	161 ± 3	403 ± 117
NADH	0.05 ± 0.01	4.84 ± 0.09	155 ± 3	3389 ± 694

Note. NAD^+ and NADH kinase activity was assayed as described in Materials and methods with different concentrations of ATP (0.01–10 mM) and NAD^+ (0.1–12 mM) or NADH (0.01–4 mM). Values are expressed as mean ± S.D. of three independent experiments.

Table 2
Phosphoryl donor specificity of NADH kinase.[a]

Phosphoryl donor[b]	Relative activity (%)	Phosphoryl donor[b]	Relative activity (%)
ATP	100	Glucose-6-Phosphate	ND
GTP	102	Phosphoenolpyruvate	ND
CTP	74	Pyrophosphate	ND
UTP	69	Metaphosphate	ND
TTP	50	Trimetaphosphate	ND
ADP	13	Hexametaphosphate	ND
dATP	103	Polyphosphate	ND
AMP	ND	Tripolyphosphate	ND
CMP	ND		

[a] Assays were performed as described in Materials and methods, in the presence of 100 mM Tris–HCl (pH 7.5), 2 mM NADH, 5 mM $MgCl_2$ and 5 mM ATP.
[b] The final concentration used was 5 mM, except for metaphosphate and polyphosphate, for which the final concentration was 2 mg/ml. The activity is shown in percentage (%) relative to that toward ATP. ND, not detected.

4. Discussion

NAD+ is a cofactor with vital dual functions involved in both energy and signal transduction [39]. Its phosphorylated form NADP+ is a key molecule in most reductive biosynthetic reactions and cellular defense against oxidative stress [40]. NAD(H) and NADP(H) are largely involved in catabolic and anabolic reactions, respectively. Furthermore, the ratio of NAD(H)/NADP(H) is a triggering signal for many signal transduction and intracellular redox reaction regulation [41]. Since NAD kinase is the sole enzyme that can phosphorylate NAD+ to form NADP+ in the presence of ATP and magnesium in both prokaryotes and eukaryotes, it plays a pivotal role in NADP-dependent pathways.

Genome survey revealed the presence of pathway responsible for NADP(H) biosynthesis in *E. histolytica*. This enteric human protozoan pathogen possesses all the enzymes necessary to synthesize NADP+/NADPH from nicotinate (Fig. 6). However, due to lack of understanding of enzymological and physiological properties of Nadhk, it remained unknown how NADP(H) biosynthesis is regulated and what its roles are on other metabolic pathways that require NADP(H) as a cofactor in *E. histolytica*. Our enzymological characterization of EhNadhk showed remarkable differences from mammalian counterpart (see below).

Table 3
Effects of metal ions on the activity of NADH kinase.[a]

Metal[b]	Relative activity (%)
None	ND
$MgCl_2$	100
$FeCl_2$	83
$CaCl_2$	43
$CoCl_2$	36
$MnCl_2$	15
$ZnCl_2$	10
$NiCl_2$	6
$CuCl_2$	2
LiCl	ND
NaCl	ND
KCl	ND

[a] Assays were performed as described in Materials and methods, in the presence of 100 mM Tris–HCl (pH 7.5), 2 mM NADH and 5 mM ATP.
[b] The concentration of cations used was 5 mM. The activity is shown in percentage (%) relative to that measured in the presence of $MgCl_2$. ND, not detected.

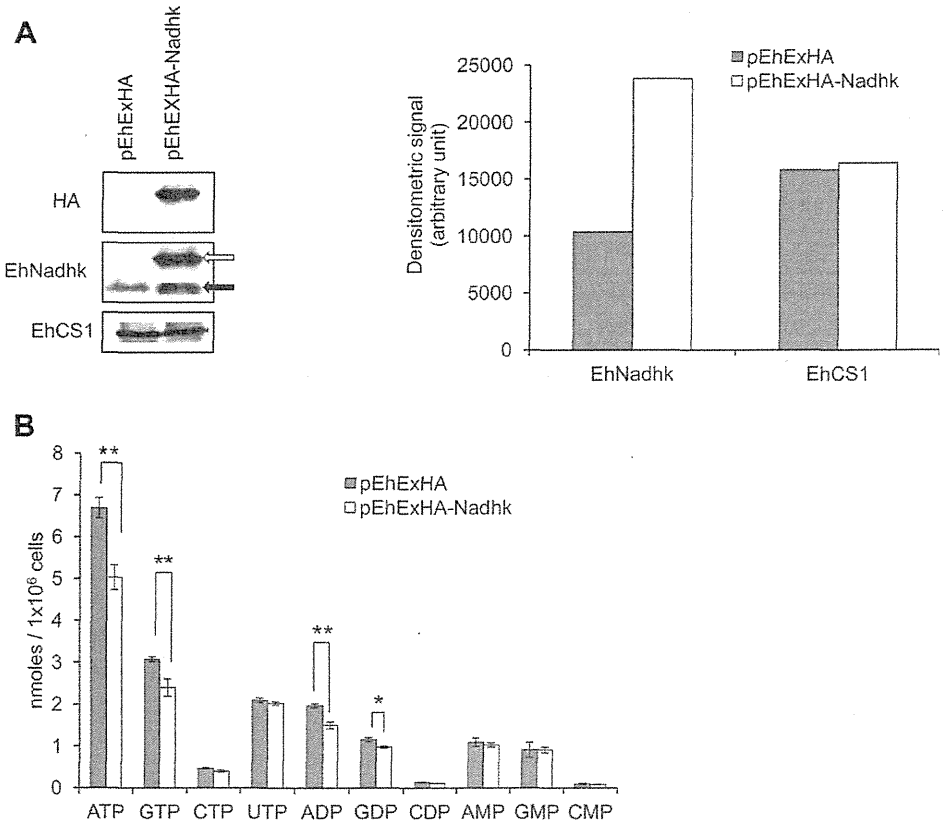

Fig. 4. Analysis of phenotypes of EhNadhk-overproducing transformant. A, Immunoblot analysis. Approximately 40 μg of total lysate from the transformant expressing HA-tagged EhNadhk (pEhExHA-Nadhk) and control strain (pEhExHA) was electrophoresed on a SDS-PAGE gel under reducing conditions and subjected to immunoblot analysis using anti-EhNadhk, anti-HA, and anti-EhCS1 antibodies. Black and white arrows indicate endogenous and HA-tagged EhNadhk, respectively. The densitometric quantification of the reacted bands, shown in the *right graph*, was performed by Image J software, and the level of EhNadhk and EhCS1 proteins was expressed in arbitrary units. B, Change in the nucleoside mono-, di-, and triphosphate levels by overexpression of EhNadhk. Data are shown as means ± S.D. Statistical comparisons were made by Student's *t* test (*$P < 0.05$, **$P < 0.01$).

Sequence comparison of EhNadhk with functionally characterized NAD kinase led to the identification of the well-conserved domain I, NE/D motif, and conserved region II (Fig. 1). Conserved domain I contains the motif GGDG, which has been previously demonstrated to be part of the ATP-binding site in 6-phosphofructokinase by three-dimensional structure analysis, and mutagenesis studies have also indicated its involvement in nucleotide binding in diacylglyceride kinase and sphingosine kinase [42]. Indeed, site-directed mutagenesis experiments performed on the *M. tuberculosis* NAD kinase GGDG sequence led to enzyme inactivation, confirming its importance in catalysis [43]. The aspartate residue of the GGDG motif may also play a role in abstracting a proton from NAD+ to activate the phosphoacceptor [43]. Conserved domain II is unique and specific to all NAD kinases so far identified. Like domain I, it contains multiple conserved glycine residues, suggesting the presence of loops coordinating nucleotide binding, as found in many nucleotide-binding enzymes [43,44]. The presence of a polar amino acid or glycine residue, but not a charged or hydrophobic amino acid residue, in the position corresponding to Gly-187 in *M. tuberculosis* NAD kinase is one of the structural determinants of phosphoryl acceptor specificity between NAD kinase and NAD(H) kinase [45]. EhNadhk contains Cys-146, which is a polar and neutral amino acid, at this position, suggesting that EhNadh kinase likely phosphorylates both NAD+ and NADH (Fig. 1).

Our repeated attempts to create a transformant in which EhNadhk expression was repressed by epigenetic gene silencing [30] failed (data not shown), suggesting the essentiality of the gene. Together with the essentiality of NAD(H) kinase demonstrated in both prokaryotes and yeast [8,13], our data support the premise that NAD(H) kinase represents a rational novel target for anti-amebic drugs. This premise is reinforced by the remarkable biochemical differences between amebic and human NAD(H) kinase demonstrated in this study, despite the protein being highly conserved in all organisms. Amebic and human NAD(H) kinase largely differ in size (43 vs 30 kDa) and show only 18% sequence similarity (Fig. 1), which was further supported with phyologentic analysis (Fig. 2). *E. histolytica* NADH kinase phosphorylates both NAD+ and NADH with marked preference to NADH (Table 1), whereas the human counterpart preferentially phosphorylates NAD+ [46].

To understand the physiological roles of *E. histolytica* NADH kinase, we generated a transformant that overexpressed Nadhk (Fig. 4A). Overexpression of this enzyme resulted in an increase in NADP+, NADPH, and a decrease in NAD+ concentrations. However, decrease in NADH concentration was marginal and statistically insignificant (Fig. 5B). Since EhNadk phosphorylates preferentially NADH to NAD+ (Table 1), this observation was unexpected. This suggests that NADH utilized by EhNadk may be immediately replenished by compensatory enzymes, e.g., NAD+-specific dehydrogenase, as NADH concentration needs to be tightly regulated. Alternatively, overexpression of EhNadhk affected in vivo partial velocities of the enzyme depending on the intracellular concentrations of NAD+/NADH. It is also possible that the increase in NADPH concentration was not due to the conversion of NADH, but

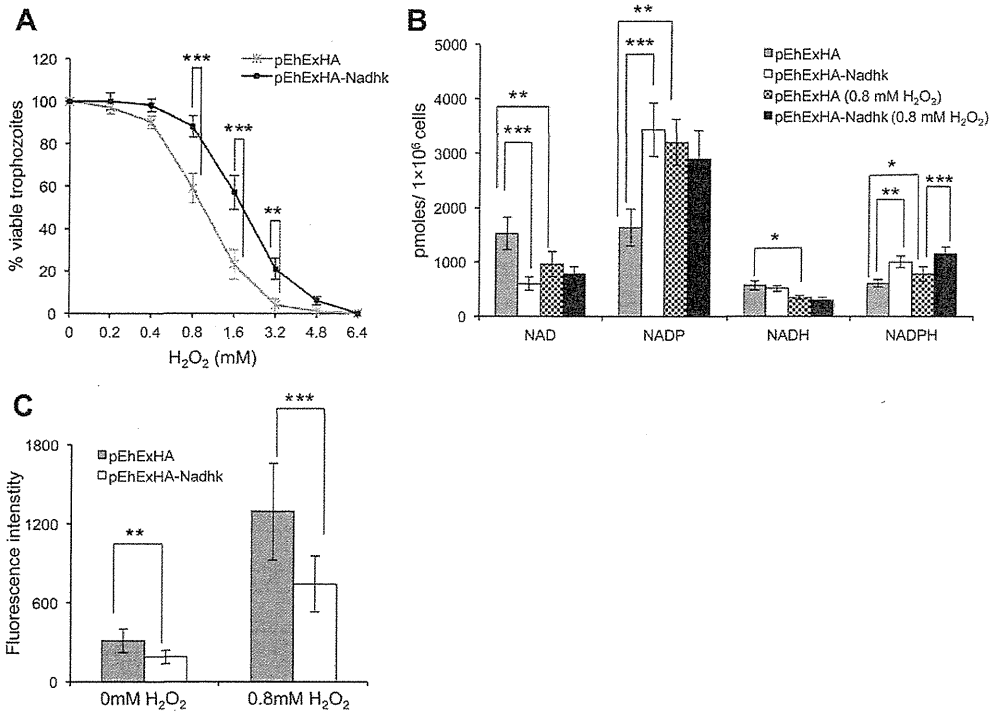

Fig. 5. Changes in the sensitivity of *E. histolytica* toward oxidative stress by overexpression of EhNadhk. A. Effect of EhNadhk expression on cell viability upon H_2O_2 treatment. Cells were exposed to different concentrations of H_2O_2. Cell viability was determined 12 h after the treatment. Values are presented as % of untreated control cells and represent the mean ± S.D. of three independent experiments conducted in triplicate. Statistical comparisons were made by Student's *t* test (**$P < 0.01$, ***$P < 0.001$). B. Nicotinamide nucleotide pools in control and overexpressing EhNadhk cells, with and without 0.8 mM H_2O_2 treatment for 12 h. Error bars represent the S.D. of three independent experiments. Statistical comparisons were made by Student's *t* test (*$P < 0.05$, **$P < 0.01$, ***$P < 0.001$). C. Influence of EhNadhk activity on the intracellular ROS levels. Cells were treated with 0.8 mM H_2O_2 for 12 h and then incubated with dye 2′,7′-DCF-DA for 30 min. The intracellular ROS levels were quantified by determination of DCF fluorescence. Results were normalized with cell numbers and presented relative to untreated control cells. The mean ± S.D. of three independent experiments performed in triplicate is shown. Statistical comparisons were made by Student's *t* test (**$P < 0.01$, ***$P < 0.001$).

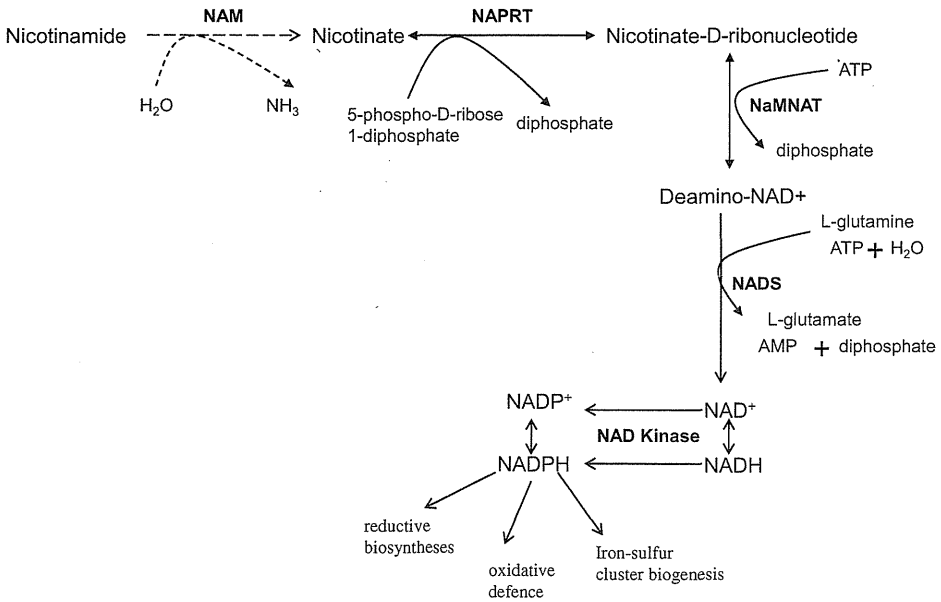

Fig. 6. Presumed NADP synthesis pathway in *E. histolytica*. Solid lines represent the steps catalyzed by the enzymes whose encoding genes are present in the genome, whereas dashed lines indicate those likely absent in the genome. Abbreviations are: NAM, nicotinamidase; NAPRT, nicotinate phosphoribosyltransferase; NaMNAT, nicotinate mononucleotide adenyltransferase; NADS, NAD synthetase.

increased activity of unknown NADP+-dependent enzymes. It has been previously shown that the overexpression of human NAD kinase, which prefers NAD+ to NADH, almost exclusively influenced NADPH without notably affecting NADP+, NAD+, and NADH concentrations [47].

E. histolytica, which is anaerobic or microaerophilic, encounters a high-oxygen environment during colonization and tissue invasion [48]. The parasite utilizes anti-oxidative defense mechanisms, in which NADPH-dependent reactions [49] are involved, to overcome oxygenated conditions [27]. Upon oxidative stress response in *E. histolytica* trophozoites, the level of NADP+ was increased approximately 2 fold, whereas NAD+ and NADH concentrations were decreased by 40% (Fig. 5B). These results may suggest that when cells were exposed to oxidative stress, the expression and activity of NAD(H) kinase and/or other enzymes involved in nicotinamide (phosphate) metabolism were increased in an effort to mitigate the oxidative stress [50]. It has previously been shown that in *Arabidopsis thaliana*, NAD(H) kinase expression is induced by 3–8 folds under oxidative stress [51]. Alternatively, these data may also be explained with the model that upon oxidative stress, synthesis of NADPH and NAD+ from NADP+ and NADH by pyridine nucleotide transhydrogenase [52] was augmented, and NADPH was then utilized for detoxification of ROS, leading to an increase in the NADP+ level.

5. Conclusion

In conclusion, we showed that NADH kinase of *E. histolytica* possesses NADH/NAD kinase activity with higher preference to NADH. This enzyme likely plays an important role in the maintenance of the intracellular redox potential and helps the parasite in response to oxidative stress. Further studies on structural properties, especially the structure of the active center, upon interactions with other ligands and potential inhibitors, should be carried out to design novel drugs targeting this enzyme. Several NAD+ analogs was previously synthesized and shown to specifically inhibit *M. tuberculosis* NAD kinase [53]. However, up to date, no effective inhibitors that suppress only microbial NAD kinase, but not human have been developed.

Acknowledgments

We thank Kumiko Nakada-Tsukui, Takashi Makiuchi and all other members of our laboratory for the technical assistance and valuable discussions. We would also like to thank Prof. Kohsaku Murata, University of Kyoto, for a human NAD kinase plasmid. This work was supported by a Grant-in-Aid for Scientific Research from the Ministry of Education, Culture, Sports, Science and Technology (MEXT) of Japan (23390099), a Grant-in-Aid for Innovative Scientific Research from MEXT (23117001, 23117005), a Grant-in-Aid on Bilateral Programs of Joint Research Projects and Seminars from Japan Society for the Promotion of Science, a Grant-in-Aid on Strategic International Research Cooperative Program from Japan Science and Technology Agency, a grant for research on emerging and re-emerging infectious diseases from the Ministry of Health, Labour and Welfare of Japan (H23-Shinkosaiko-ippan-014), a grant for research to promote the development of anti-AIDS pharmaceuticals from the Japan Health Sciences Foundation (KHA1101) to T.N. G.J. and T.N. were supported in part by the Global Center of Excellence Program for Human Metabolomic System Biology from MEXT.

References

[1] S.L. Stanley, Amoebiasis, Lancet 361 (2003) 1025–1034.
[2] World Health Organization, WHO/PAHO/UNESCO Report: a consultation with experts on amebiasis. Mexico City, Mexico 28–29 January, 1997, Epidemiol. Bull. 18 (1997) 13–14.
[3] V. Ali, T. Nozaki, Current therapeutics, their problems, and sulfur-containing-amino-acid metabolism as a novel target against infections by "amitochondriate" protozoan parasites, Clin. Microbiol. Rev. 20 (2007) 164–187.
[4] C. Wassmann, A. Hellberg, E. Tannich, I. Bruchhaus, Metronidazole resistance in the protozoan parasite *Entamoeba histolytica* is associated with increased expression of iron-containing superoxide dismutase and peroxiredoxin and decreased expression of ferredoxin 1 and flavin reductase, J. Biol. Chem. 274 (1999) 26051–26056.
[5] N. Pollak, C. Dolle, M. Ziegler, The power to reduce: pyridine nucleotides-small molecules with a multitude of functions, Biochem. J. 402 (2007) 205–218.
[6] W. Cheng, J.R. Roth, Evidence for two NAD kinases in *Salmonella typhimurium*, J. Bacteriol. 176 (1994) 4260–4268.
[7] C. Stephan, M. Renard, F. Montrichard, Evidence for the existence of two soluble NAD+ kinase isoenzymes in Euglena gracilis Z, Int. J. Biochem. Cell. Biol. 32 (2000) 855–863.
[8] P. Bieganowski, H.F. Seidle, M. Wojcik, C. Brenner, Synthetic lethal and biochemical analyses of NAD and NADH kinases in *Saccharomyces cerevisiae* establish separation of cellular functions, J. Biol. Chem. 281 (2006) 22439–22445.
[9] F. Shi, S. Kawai, S. Mori, E. Kono, K. Murata, Identification of ATP-NADH kinase isozymes and their contribution to supply of NADP(H) in *Saccharomyces cerevisiae*, FEBS J. 272 (2005) 3337–3349.
[10] Y.F. Li, F. Shi, Partial rescue of *pos5* mutants by *YEF1* and *UTR1* genes in *Saccharomyces cerevisiae*, Acta Biochim. Biophys. Sin. 38 (2006) 293–298.
[11] J. Pain, M.M. Balamurali, A. Dancis, D. Pain, Mitochondrial NADH Kinase, Pos5p, is required for efficient iron-sulfur cluster biogenesis in *Saccharomyces cerevisiae*, J. Biol. Chem. 285 (2010) 39409–39424.
[12] C.M. Sassetti, D.H. Boyd, E.J. Rubin, Genes required for mycobacterial growth defined by high-density mutagenesis, Mol. Microbiol. 48 (2003) 77–84.
[13] K. Kobayashi, S.D. Ehrlich, A. Albertini, G. Amati, K.K. Andersen, M. Arnaud, K. Asai, et al., Essential *Bacillus subtilis* genes, Proc. Natl. Acad. Sci. 100 (2003) 4678–4683.
[14] S.Y. Gerdes, M.D. Scholle, M. D'souza, A. Bernal, M.V. Baev, M. Farrell, O.V. Kurnasov, et al., From genetic footprinting to antimicrobial drug targets: examples in cofactor biosynthetic pathways, J. Bacteriol. 184 (2002) 4555–4572.
[15] J.H. Grose, L. Joss, S.F. Velick, J.R. Roth, Evidence that feedback inhibition of NAD kinase controls responses to oxidative stress, Proc. Natl. Acad. Sci. 103 (2006) 7601–7606.
[16] F. Lerner, M. Niere, A. Ludwig, M. Ziegler, Structural and functional characterization of human NAD Kinase, Biochem. Biophys. Res. Commun. 288 (2001) 69–74.
[17] G. Magni, G. Orsomando, N. Raffaelli, Structural and functional properties of NAD kinase, a key enzyme in NADP biosynthesis, Mini Rev. Med. Chem. 6 (2006) 739–746.
[18] R. Bracha, Y. Nuchamowitz, M. Anbar, D. Mirelman, Transcriptional silencing of multiple genes in trophozoites of *Entamoeba histolytica*, PLoS Pathog. 2 (2006) e48.
[19] L.S. Diamond, D.R. Harlow, C.C. Cunnick, A new medium for the axenic cultivation of *Entamoeba histolytica* and other *Entamoeba*, Trans. R Soc. Trop. Med. Hyg. 72 (1978) 431–432.
[20] J.D. Thompson, D.G. Higgins, T.J. Gibson, CLUSTAL W: improving the sensitivity of progressive multiple sequence alignment through sequence weighting, position-specific gap penalties and weight matrix choice, Nucleic Acids Res. 22 (1999) 4673–4680.
[21] A.N. Leão-Helder, A.M. Krikken, G. Gellissen, I.J. van der Klei, M. Veenhuis, J.A. Kiel, Atg21p is essential for macropexophagy and microautophagy in the yeast *Hansenula polymorpha*, FEBS Lett. 577 (2004) 491–495.
[22] S. Kumar, K. Tamura, I.B. Jakobsen, M. Nei, MEGA2: molecular evolutionary genetics analysis software, Bioinformatics 17 (2001) 1244–1245.
[23] J. Sambrook, D.W. Russell, Molecular Cloning: A Laboratory Manual, third ed. Cold Spring Harbor Laboratory Press, Cold Spring Harbor, NY, 2001.
[24] T. Nozaki, T. Asai, S. Kobayashi, F. Ikegami, M. Noji, K. Saito, T. Takeuchi, Molecular cloning and characterization of the genes encoding two isoforms of cysteine synthase in the enteric protozoan parasite, *Entamoeba histolytica*, Mol. Biochem. Parasitol. 97 (1998) 33–44.
[25] M.M. Bradford, A rapid and sensitive method for the quantitation of microgram quantities of protein utilizing the principle of protein–dye binding, Anal. Biochem. 72 (1976) 248–254.
[26] S. Kawai, S. Mori, T. Mukai, S. Suzuki, W. Hashimoto, T. Tamada, K. Murata, Inorganic polyphosphate/ATP-NAD kinase of Micrococcus flavus and *Mycobacterium tuberculosis* H37Rv, Biochem. Biophys. Res. Commun. 276 (2000) 57–63.
[27] G. Jeelani, A. Husain, D. Sato, V. Ali, M. Suematsu, T. Soga, T. Nozaki, Two atypical L-cysteine-regulated NADPH-dependent oxidoreductases involved in redox maintenance, L-cystine and iron reduction, and metronidazole activation in the enteric protozoan *Entamoeba histolytica*, J. Biol. Chem. 285 (2010) 26889–26899.
[28] K. Nakada-Tsukui, H. Okada, B.N. Mitra, T. Nozaki, Phosphatidylinositol-phosphates mediate cytoskeletal reorganization during phagocytosis via a unique modular protein consisting of RhoGEF/DH and FYVE domains in the parasitic protozoon *Entamoeba histolytica*, Cell. Microbiol. 11 (2009) 1471–1491.
[29] T. Nozaki, T. Asai, L.B. Sanchez, S. Kobayashi, M. Nakazawa, T. Takeuchi, Characterization of the gene encoding serine acetyltransferase, a regulated enzyme of cysteine biosynthesis from the protist parasites *Entamoeba*

histolytica and *Entamoeba dispar*. Regulation and possible function of the cysteine biosynthetic pathway in Entamoeba, J. Biol. Chem. 274 (1999) 32445–32452.
[30] H. Zhang, H. Alramini, V. Tran, U. Singh, Nucleus-localized antisense small RNAs with 5'-polyphosphate termini regulate long term transcriptional gene silencing in *Entamoeba histolytica* G3 strain, J. Biol. Chem. 286 (2011) 44467–44479.
[31] A. Husain, G. Jeelani, D. Sato, T. Nozaki, Global analysis of gene expression in response to L-cysteine deprivation in the anaerobic protozoan parasite *Entamoeba histolytica*, BMC Genomics 12 (2011) 275.
[32] J. Bai, A.M. Rodriguez, J.A. Melendez, A.I. Cederbaum, Overexpression of catalase in cytosolic or mitochondrial compartment protects HepG2 cells against oxidative injury, J. Biol. Chem. 274 (1999) 26217–26224.
[33] A. Husain, D. Sato, G. Jeelani, F. Mi-ichi, V. Ali, M. Suematsu, T. Soga, T. Nozaki, Metabolome analysis revealed increase in S-methylcysteine and phosphatidyl isopropanolamine synthesis upon L-cysteine deprivation in the anaerobic protozoan parasite *Entamoeba histolytica*, J. Biol. Chem. 285 (2010) 39160–39170.
[34] Y. Ohashi, A. Hirayama, T. Ishikawa, S. Nakamura, K. Shimizu, Y. Ueno, M. Tomita, T. Soga, Depiction of metabolome changes in histidine-starved *Escherichia coli* by CE-TOFMS, Mol. Biosyst. 4 (2008) 135–147.
[35] M. Tokoro, T. Asai, S. Kobayashi, T. Takeuchi, T. Nozaki, Identification and characterization of two isoenzymes of methionine gamma-lyase from *Entamoeba histolytica*: a key enzyme of sulfur-amino acid degradation in an anaerobic parasitic protist that lacks forward and reverse trans-sulfuration pathways, J. Biol. Chem. 278 (2003) 42717–42727.
[36] S. Garavaglia, N. Raffaelli, L. Finaurini, G. Magni, M. Rizzi, A novel fold revealed by *Mycobacterium tuberculosis* NAD kinase, a key allosteric enzyme in NADP biosynthesis, J. Biol. Chem. 279 (2004) 40980–40986.
[37] S. Kawai, S. Mori, T. Mukai, W. Hashimoto, K. Murata, Molecular characterization of *Escherichia coli* NAD kinase, Eur. J. Biochem. 268 (2001) 4359–4365.
[38] U.C. Alsmark, T. Sicheritz-Ponten, P.G. Foster, R.P. Hirt, T.M. Embley, Horizontal gene transfer in eukaryotic parasites: a case study of *Entamoeba histolytica* and *Trichomonas vaginalis*, Methods Mol. Biol. 532 (2009) 489–500.
[39] F. Berger, M.H. Ramirez-Hernandez, M. Ziegler, The new life of a centenarian: signalling functions of NAD(P), Trends Biochem. Sci. 29 (2004) 111–118.
[40] C.E. Outten, V.C. Culotta, A novel NADH kinase is the mitochondrial source of NADPH in *Saccharomyces cerevisiae*, EMBO J. 22 (2003) 2015–2024.
[41] S. Kawai, K. Murata, Structure and function of NAD kinase and NADP phosphatase: key enzymes that regulate the intracellular balance of NAD(H) and NADP(H), Biosci. Biotechnol. Biochem. 72 (2008) 919–930.
[42] G. Labesse, D. Douget, L. Assairi, A. Gilles, Diacylglyceride kinases, sphingosine kinases and NAD kinases: distant relatives of 6-phosphofructokinases, Trends Biochem. Sci. 27 (2002) 273–275.
[43] N. Raffaelli, L. Finaurini, F. Mazzola, L. Pucci, L. Sorci, A. Amici, G. Magni, Characterization of *Mycobacterium tuberculosis* NAD Kinase: functional analysis of the full-length enzyme by site-directed mutagenesis, Biochemistry 43 (2004) 7610–7617.
[44] M. Saraste, P.R. Sibbald, A. Wittinghofer, The P-loops: a common motif in ATP- and GTP-binding proteins, Trends Biochem. Sci. 15 (1990) 430–434.
[45] S. Mori, S. Kawai, F. Shi, B. Mikami, K. Murata, Molecular conversion of NAD kinase to NADH kinase through single amino acid residue substitution, J. Biol. Chem. 280 (2005) 24104–24112.
[46] K. Ohashi, S. Kawai, M. Koshimizu, K. Murata, NADPH regulates human NAD kinase, a $NADP^+$-biosynthetic enzyme, Mol. Cell. Biochem. 355 (2011) 57–64.
[47] N. Pollak, M. Niere, M. Ziegler, NAD kinase levels control the NADPH concentration in human cells, J. Biol. Chem. 282 (2007) 33562–33571.
[48] M.A. Akbar, N.S. Chatterjee, P. Sen, A. Debnath, A. Pal, T. Bera, P. Das, Genes induced by a high-oxygen environment in *Entamoeba histolytica*, Mol. Biochem. Parasitol. 133 (2004) 187–196.
[49] F. Shi, Y. Li, Y. Li, X. Wang, Molecular properties, functions, and potential applications of NAD kinases, Acta Biochim. Biophys. Sin 41 (2009) 352–361.
[50] R. Singh, J. Lemire, R.J. Mailloux, V.D. Appanna, Oxidative stress evokes a metabolic adaptation that favors increased NADPH synthesis and decreased NADH production in *Pseudomonas fluorescens*, J. Bacteriol. 189 (2007) 6665–6675.
[51] J.G. Berrin, O. Pierrugues, C. Brutesco, B. Alonso, J.L. Montillet, D. Roby, M. Kazmaier, Stress induces the expression of AtNADK-1, a gene encoding a NAD(H) kinase in *Arabidopsis thaliana*, Mol. Genet. Genomics 273 (2005) 10–19.
[52] M.A. Yousuf, F. Mi-ichi, K. Nakada-Tsukui, T. Nozaki, Localization and targeting of an unusual pyridine nucleotide transhydrogenase in *Entamoeba histolytica*, Eukaryot. Cell. 9 (2010) 926–933.
[53] L. Bonnac, L. Chen, R. Pathak, G. Gao, Q. Ming, E. Bennett, K. Felczak, M. Kullberg, S.E. Patterson, F. Mazzola, G. Magni, K.W. Pankiewicz, Probing binding requirements of NAD kinase with modified substrate (NAD) analogues, Bioorg. Med. Chem. Lett. 17 (2007) 1512–1515.

SCIENTIFIC REPORTS

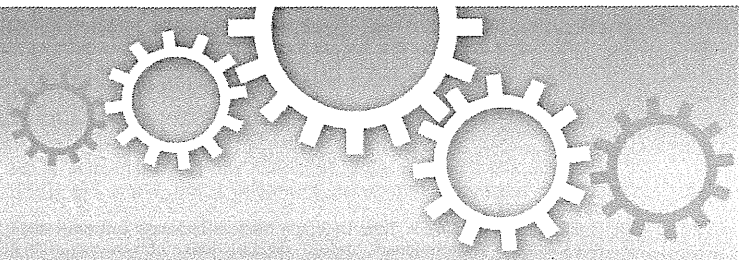

OPEN

SUBJECT AREAS:
EVOLUTION
PARASITOLOGY
MITOCHONDRIA
MOLECULAR EVOLUTION

Received
10 October 2012

Accepted
27 December 2012

Published
24 January 2013

Correspondence and requests for materials should be addressed to T.N. (nozaki@niid.go.jp)

* Current address: Department of Biomolecular Sciences, Faculty of Medicine, Saga University, 5-1-1 Nabeshima, Saga 849-8501, Japan

Novel TPR-containing subunit of TOM complex functions as cytosolic receptor for *Entamoeba* mitosomal transport

Takashi Makiuchi[1,2], Fumika Mi-ichi[1]*, Kumiko Nakada-Tsukui[1] & Tomoyoshi Nozaki[1,3]

[1]Department of Parasitology, National Institute of Infectious Diseases, 1-23-1 Toyama, Shinjuku-ku, Tokyo 162-8640, Japan, [2]Kitasato Institute for Life Sciences and Graduate School of Infection Control Sciences, Kitasato University, Minato-ku, Tokyo 108-8641, Japan, [3]Graduate School of Life and Environmental Sciences, University of Tsukuba, 1-1-1 Tennodai, Tsukuba, Ibaraki 305-8572, Japan.

Under anaerobic environments, the mitochondria have undergone remarkable reduction and transformation into highly reduced structures, referred as *m*itochondrion-related *o*rganelles (MROs), which include mitosomes and hydrogenosomes. In agreement with the concept of reductive evolution, mitosomes of *Entamoeba histolytica* lack most of the components of the TOM (*t*ranslocase of the *o*uter *m*itochondrial membrane) complex, which is required for the targeting and membrane translocation of preproteins into the canonical aerobic mitochondria. Here we showed, in *E. histolytica* mitosomes, the presence of a 600-kDa TOM complex composed of Tom40, a conserved pore-forming subunit, and Tom60, a novel lineage-specific receptor protein. Tom60, containing multiple tetratricopeptide repeats, is localized to the mitosomal outer membrane and the cytosol, and serves as a receptor of both mitosomal matrix and membrane preproteins. Our data indicate that *Entamoeba* has invented a novel lineage-specific shuttle receptor of the TOM complex as a consequence of adaptation to an anaerobic environment.

Mitochondria are highly divergent structures in eukaryotes, and often reveal degenerate morphology, function, and components in eukaryotes that have been adapted in anoxic or hypoxic environments. Such degenerated mitochondria with reduced or no organellar genome are called mitochondrion-related organelles (MROs), which include mitosomes and hydrogenosomes. While the minimal common function of MROs is still in debate[1–6], protein import of nuclear-encoded proteins into MROs is indispensable for the organisms that possess MROs. All organisms possessing MRO that have been investigated so far, indeed retain at least a gene encoding the core translocation channel Tom40 of the TOM (*T*ranslocase of the *O*uter membrane of *M*itochondria)[7–11]. However, in agreement with the concept of reductive evolution, other components of the canonical aerobic mitochondria such as subunits of TOM, SAM (*S*orting and *A*ssembly *M*achinery), TIM (*T*ranslocase of the *I*nner membrane of *M*itochondria), and small TIM complexes[8,12,13] are often missing in MROs. These data imply two possible scenarios of evolution of mitochondrial protein import: the majority of the import machinery of MROs has been secondarily lost[7,8], or the transport machinery or subunits were replaced with unique and possibly lineage-specific components[14].

The TOM complex is involved in the initial process of the import of nuclear-encoded mitochondrial preproteins into the mitochondria. Remarkable variation exists in the architecture of TOM complexes among eukaryotic lineages. In yeast and mammals, the translocation channel (Tom40), membrane-anchored receptors for the recognition of a targeting signal in preproteins (Tom22, Tom20, and Tom70), and accessory subunits (Tom5, Tom6, and Tom7) consist the TOM complex[15,16]. In plants, an 8-kDa truncated form of Tom22 serves as translocase[17] and chloroplast import receptor Toc64 homolog functions as a TOM component[18], while in trypanosomes, Tom40 appears to be replaced by Omp85 of archaic origin[19]. Tom20, a presequence binding receptor appeared to have independently evolved from two distinct ancestral genes in the animal and plant lineages[20]. Therefore, the investigation of the TOM complex may shed light on the evolution of the protein import machinery of endosymbiont-derived organelles.

Entamoeba histolytica is an anaerobic unicellular parasite, and causes hemorrhagic dysentery and extra intestinal abscesses that are responsible for an estimated 100,000 deaths in endemic areas annually[21]. This parasite possesses mitosomes, and is a good representative of mitochondrial diversification. *Entamoeba* MRO contains the sulfate activation pathway, which has been so far identified only in this organism[9]. Moreover, it lacks a

genome[22], has no membrane potential[22,23], and is devoid of an import system using the canonical transit peptide[9]. Furthermore, *E. histolytica* has none of the homologous subunits of the TOM complex except Tom40[9,13]. This fact, more specifically the lack of Tom20 and Tom70 receptors, suggests that import of mitosomal proteins does not depend on receptor recognition in *Entamoeba*, or that *Entamoeba* possesses an unprecedented receptor subunit undetectable by currently available *in silico* analysis. Here we show that the TOM complex in the *E. histolytica* mitosomes contains a lineage specific subunit, designated Tom60, which is associated with Tom40. Repression of Tom40 or Tom60 by gene silencing shows defects in protein import to mitosomes, and consequently retardation of proliferation. Tom60 is distributed to both the periphery of the mitosomal outer membrane and the cytosol. Moreover, our data strongly suggest that Tom60 is capable to bind *in vitro* to both mitosomal matrix proteins and membrane proteins.

Results

Demonstration of Tom40 localization on *Entamoeba* mitosomes. As we aimed to characterize TOM complex from *Entamoeba*, we first established an *E. histolytica* cell line expressing hemagglutinin (HA)-tagged *E. histolytica* Tom40 (EhTom40) at the carboxyl terminus (Tom40-HA). To verify the expression and mitosomal localization of Tom40-HA, we fractionated lysates from Tom40-HA-expressing trophozoites by two rounds of Percoll gradient ultracentrifugation and analyzed the fractions by immunoblot with anti-HA antibody and anti-Cpn60 antiserum[9]. Cpn60 served as a canonical mitosomal marker. The banding pattern of Tom40-HA among fractions was similar to that of Cpn60 (Supplementary Fig. S1). Next, we carried out the immunofluorescence assay (IFA) using anti-HA antibody and anti-Cpn60 antiserum (Supplementary Fig. S2). Fluorescence signals of Tom40-HA were observed as dotted pattern and were merged with fluorescence signals of Cpn60, suggesting that EhTom40 is localized in mitosomes. Moreover, mitosomal localization of EhTom40 was also supported by immunoelectron microscopy (immuno-EM) (Supplementary Fig. S3) showing that Tom40-HA is concentrated on mitosomal outer membranes.

Identification of 600-kDa *Entamoeba* TOM complex and a novel subunit Tom60. The TOM complex exists in yeast as a ~400-kDa complex, composed of Tom40, Tom22, Tom5, Tom6, and Tom7[24]. To see if *Entamoeba* mitosomes contain TOM complex, and if so, to isolate the whole complex and identify proteins interacting with EhTom40, we investigated an EhTom40-containing complex by blue native polyacrylamide gel electrophoresis (BN-PAGE) followed by immunoblot with anti-HA antibody. Immunoblot analysis of the 100,000 × *g* organelle-enriched fraction of Tom40-HA-expressing trophozoites with anti-HA antibody showed a 600-kDa band (Fig. 1a). To isolate and identify proteins that are associated with the 600-kDa band, the complex was immunoprecipitated with anti-HA antibody (Fig. 1b) and electrophoresed on SDS-PAGE under reducing conditions. A band of approximately 60-kDa in size was detected exclusively in samples co-immunoprecipitated with lysates from the Tom40-HA-expressing trophozoites (Fig. 1c). The band was subjected to liquid chromatography-tandem mass spectrometric analysis (LC-MS/MS), identified to be XP_657124 (Supplementary Fig. S4 and S5, and Supplementary Table S1A), and designated as *E. histolytica* Tom60 (EhTom60). EhTom60 was also detected by LC-MS/MS analysis of the 600-kDa complex (Supplementary Table S1B). The protein was previously identified in our mitosome proteome[9].

Lineage specific distribution of Tom60. Tom60 appears to be uniquely present in the genus. Tom60 orthologs were found in *E. dispar* and *E. invadens* (EDI_218540 and EIN_149090, respectively)

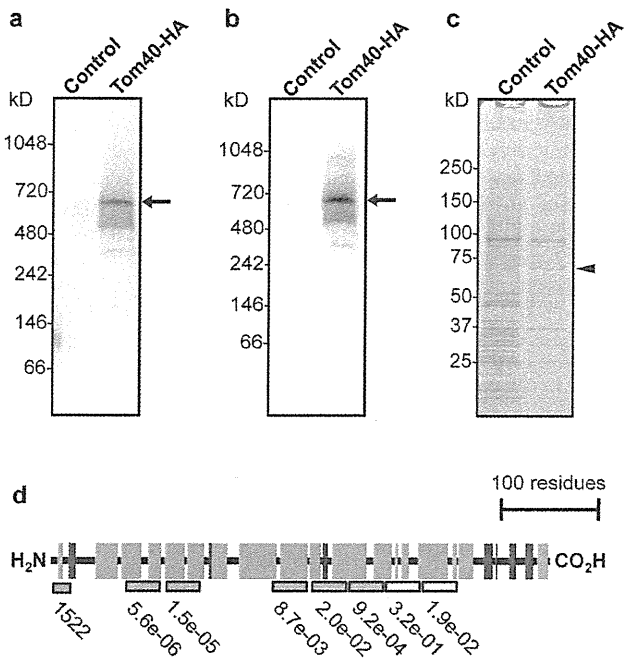

Figure 1 | Identification of the *Entamoeba* TOM complex and its novel subunit. (a), The TOM complex demonstrated by BN-PAGE and immunoblot analysis. (b), Immunoprecipitation of the TOM complex (arrows) from Tom40-HA transformant by BN-PAGE and immunoblot analysis with anti-HA antibody. (c), SDS-PAGE and silver stain of immunoprecipitated TOM complex from Tom40-HA. Arrowhead indicates Tom60. (d), Prediction of the secondary structure and the domain organization of EhTom60. Gray box indicates the hydrophobic cluster, while pink and yellow boxes depict putative tetratricopeptide repeats (TPRs) conserved among genus *Entamoeba* or those specific to *E. histolytica*, respectively. Probability and *E*-value are shown (Supplementary Fig. S4). Green and blue boxes indicate α-helices and β-strands, respectively, predicted by PSIPRED (Supplementary Fig. S6).

(Supplementary Fig. S4), whereas they were not identified in bacteria, archaea, and other eukaryotes. Among amoebozoan organisms, we confirmed by BLAST search (using the threshold of *E*-value < 0.1) that a Tom60 homolog is absent in the *Dictyostelium discoideum* (dictyBase: http://dictybase.org/) and *Acanthamoeba catellani* (https://www.hgsc.bcm.edu/content/acanthamoeba-castellani-neff) genomes, and the transcriptome of *Mastigamoeba balamuthi* (Spears, C. and Roger, A., personal communication).

In silico analyses indicate that *Entamoeba* Tom60 contains putative tetratricopeptide repeats (TPRs)[25] and an amino-terminal hydrophobic cluster (Fig. 1d and Supplementary Fig. S4). TPRs are implicated in protein-protein interactions, and are also present in Tom20 and Tom70, which are membrane-spanning receptors for mitochondrial import[26], suggesting that *Entamoeba* Tom60 may be a receptor for mitosomal import. However, in contrast to the above-mentioned TPR-containing mitochondrial receptors, which consist of only α-helices, *Entamoeba* Tom60 appears to contain β-strands, based on the secondary structure prediction by PSIPRED (http://bioinf.cs.ucl.ac.uk/psipred/) (Fig. 1d and Supplementary Fig. S6). The predicted structural differences argue against the premise that *Entamoeba* Tom60 has a common evolutionary origin with Tom20 and Tom70.

Furthermore, phylogenetic analyses of TPR elements from 23 yeast proteins, plant Toc64, human Tom34 (Supplementary Table S2), 36 *D. discoideum* proteins (Supplementary Table S3), and 28 TPR-containing proteins from *Entamoeba* (Supplementary

Table S4), showed that TPRs of *Entamoeba* Tom60s have no significant affinity with TPRs from other proteins. Therefore, we conclude that *Entamoeba* Tom60 is a genus-specific protein.

Localization and membrane topology of Tom60. We confirmed by IFA the mitosomal localization of Tom60 in an *E. histolytica* cell line expressing Tom40-Myc and Tom60-HA. EhTom40, EhTom60, and APS kinase[9] (APSK; XP_656278) were colocalized and concentrated in the mitosomes (Fig. 2a). However, faint cytosolic signals were also detected for EhTom60 (data not shown). Next, to verify localization, cellular fractionation of lysates was performed, followed by immunoblot analysis. EhTom60 was detected in both the 100,000 × *g* organelle fraction and the soluble supernatant fraction, suggesting that EhTom60 is present in both mitosomes and the cytosol. We next investigated the topology of EhTom60, EhTom40, and other mitosomal proteins by examining their sensitivity to proteinase K treatment followed by immunoblot analysis (Fig. 2b). Proteinase K sensitivity increased in the order of APSK-HA, AAC-HA (inner membrane protein[23,27])/Tom40-HA, and Tom60-HA (Fig. 2b). Furthermore, sodium carbonate treatment, which liberates soluble and peripheral membrane proteins from organelles[28], decreased the amount of organelle-associated Tom60-HA and increased that of soluble Tom60-HA, while Tom40-HA and CPBF1-HA (single-membrane spanning protein)[29] remained in the pellet fraction after the treatment (Fig. 2b, left and Fig. 2c). These data demonstrate that EhTom60 is a cytosolic protein which can associate with EhTom40 on the surface of the mitosomal outer membrane.

Phenotypes of *Tom40*- and *Tom60*-gene silencing. The importance of mitosomal matrix proteins, i.e., ATP sulfurylase (AS; XP_653570), APSK, inorganic pyrophosphatase (IPP; XP_649445), Cpn60, and AAC for *E. histolytica* proliferation was previously verified by gene silencing[27]. To demonstrate the biological importance of the mitosomal import machinery per se, we established *E. histolytica* strains in which *EhTom40* and *EhTom60* genes were silenced. Gene silencing was verified by quantitative real-time PCR (Fig. 3a). Repression of *EhTom40* and *EhTom60* genes caused a decrease in the transport of mitosomal matrix proteins, Cpn60,

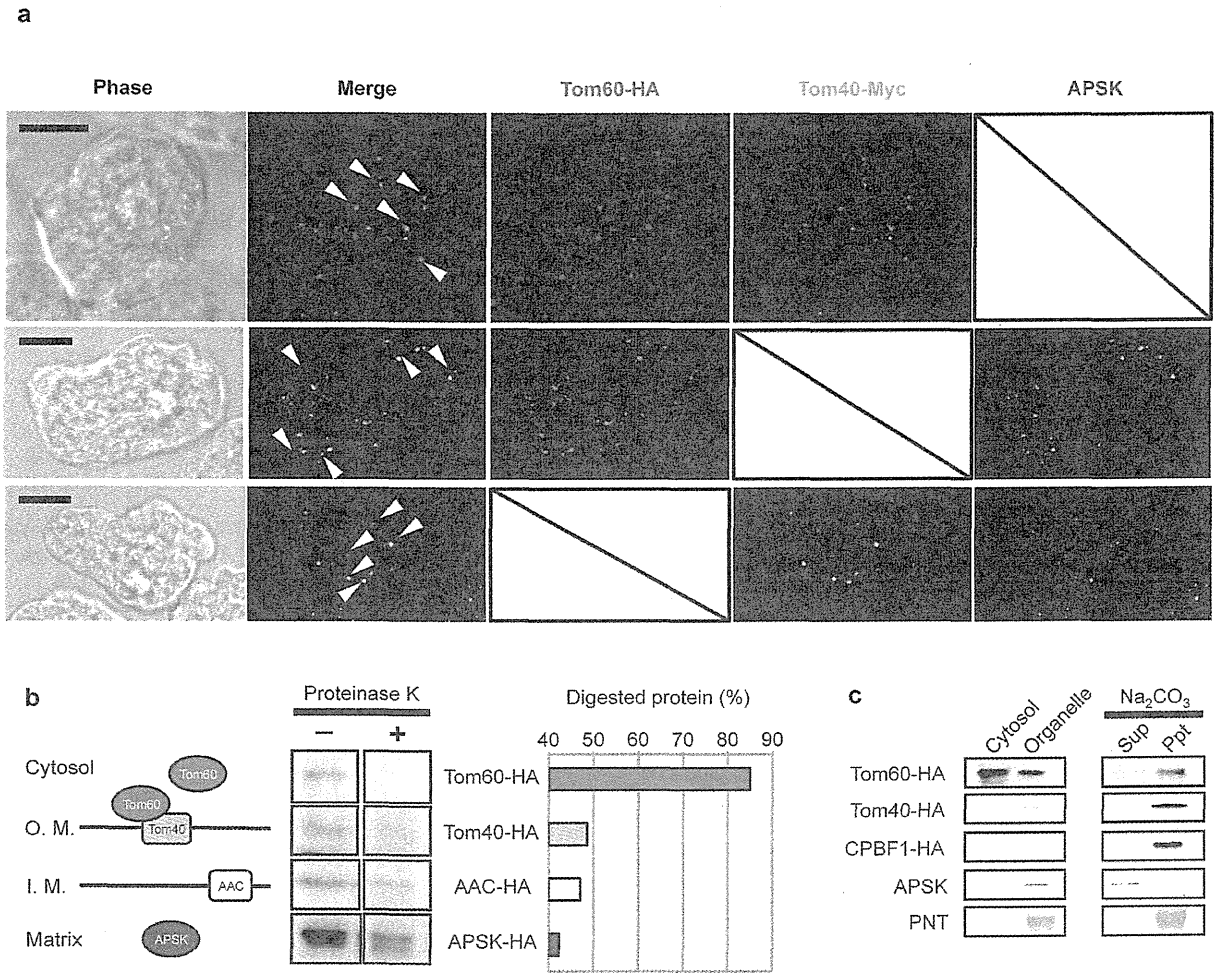

Figure 2 | Localization and topology of Tom40 and Tom60. (a), Indirect fluorescence analyses of Tom40-HA and Tom60-Myc. Anti-APSK antiserum was used as mitosomal marker. Scale bar = 10 μm. (b), Differential sensitivity of several mitosomal proteins to proteinase K treatment. Left panel shows expected topologies of Tom60, Tom40, AAC, and APSK. "O. M." and "I. M." indicate outer and inner membranes, respectively. Middle panel shows immunoblots of each organelle fraction treated (+) or untreated (−) with proteinase K. Right panel shows the ratio of digested protein to that of total undigested protein. (c), Fractionation of mitosomal components. Lysates from amoebae expressing Tom60-HA, Tom40-HA, and CPBF1 (cysteine protease binding family protein 1; XP_655218[29])-HA were fractionated. The three upper and two lower blots were reacted with anti-HA, anti-APSK, or anti-pyridine nucleotide transhydrogenase (PNT, XP_001914099[55]) antibody. CPBF1 and PNT serve as a control for single- and multi-membrane spanning proteins, respectively.

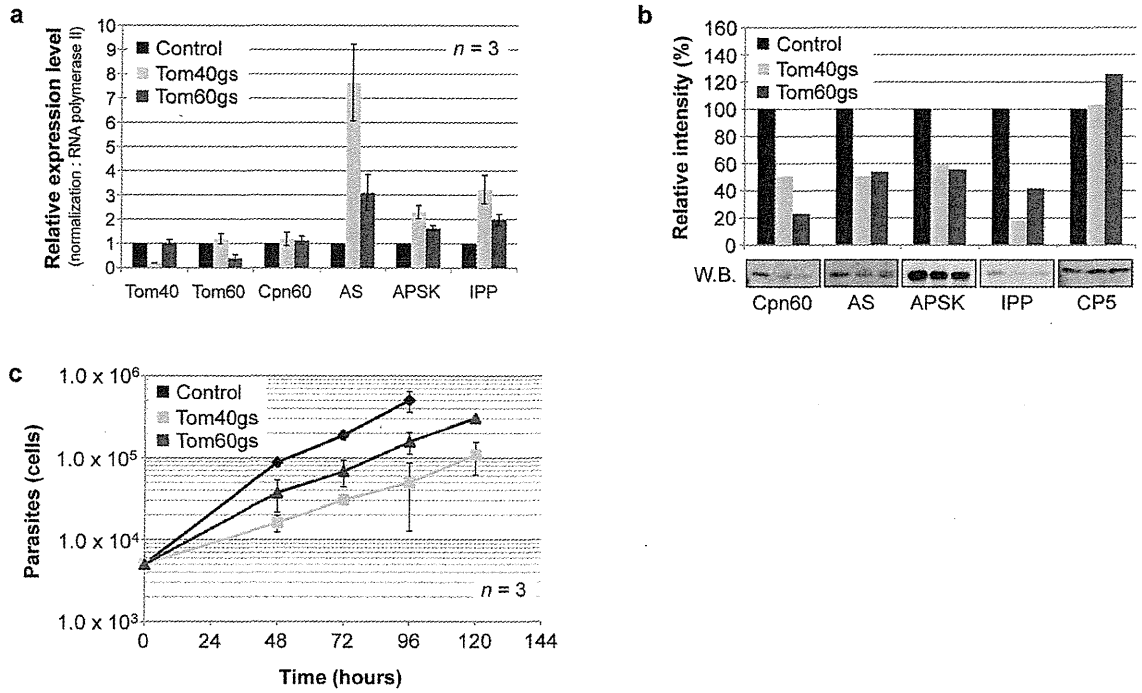

Figure 3 | Phenotypes of *Tom40*- and *Tom60*-gene silenced strain. (a), Effects on the relative mRNA expression levels of mitosomal proteins of *Tom40*- and *Tom60*-gene silencing. Error bars indicate standard deviations. (b), Effects on the amount of mitosomal proteins in organelle fractions from *Tom40*-gene silenced (gs) and Tom60gs strains. Cysteine protease 5 (CP5) was used as loading control. Relative levels of each transcript and protein are shown after normalization against control. (c), Growth kinetics of Tom40gs, Tom60gs, and control strains.

AS, APSK, and IPP (Fig. 3b). On the contrary, we observed a remarkable accumulation of AS, APSK, and IPP transcripts in *EhTom40*- and *EhTom60*-gene silenced strains (Fig. 3a). Finally, repression of *EhTom40* and *EhTom60* genes caused growth retardation when compared to control (Fig. 3c), suggesting that EhTom40 and EhTom60 are important for proliferation. These data also suggest that gene transcription of matrix proteins was upregulated by compensatory mechanisms, but was not sufficient to overcome undesirable effects caused by the repression of proteins involved in the mitosome import. Taken together, we conclude that EhTom40 and EhTom60 play essential roles in the import of matrix proteins to mitosomes.

Tom60 serves as a cytosolic receptor of mitosomal proteins. To verify whether EhTom60 functions as a receptor subunit of the TOM complex, we performed an *in vitro* binding assay, using recombinant AS and cysteine synthase isotype 3 (CS3, XP_653246; control for an irrelevant cytosolic protein) that have the FLAG-tag at the carboxyl terminus, and recombinant His-Tom60ΔN-HA, which lacks the amino-terminal hydrophobic region (a.a. 1–30) of EhTom60, and contained the His-tag at the amino terminus. We removed the amino-terminal region of EhTom60 because it negatively affected solubility of the recombinant protein. His-Tom60ΔN-HA showed a higher binding affinity towards AS-FLAG than CS3-FLAG (Fig. 4a and b; Supplementary Fig. S7). Moreover, the binding efficiency of His-Tom60ΔN-HA to AS-FLAG, but not CS3-FLAG, increased at higher KCl concentrations, which agreed well with the salt dependence of the binding between mitochondrial preproteins and the yeast Tom20[30]. These results strongly suggest that EhTom60 functions as a receptor for soluble proteins imported into the mitosomal matrix.

It has been demonstrated that in fungi, metazoa, and plants, mitochondrial transport of matrix and membrane proteins is mediated by different receptors, Tom20 and Tom70, respectively. Tom20 directly recognizes the amino-terminal presequence of soluble matrix proteins. However, Tom70 interacts with membrane preproteins directly, or indirectly via cytosolic heat shock protein 70 (Hsp70) and Hsp90 chaperones. In the latter case, Hsp70 and Hsp90 that are bound to mitochondrial membrane preproteins[31] further bind to the TPR domains of Tom70 via their conserved tetrapeptide "EEVD" motif at the carboxyl terminus[32]. We thus tested if *Entamoeba* TPR-containing Tom60 can also recognize the tetrapeptide motif present in *E. histoltyica* Hsp70 and Hsp90. His-Tom60ΔN-HA was mixed with recombinant CS3-FLAG or its engineered form (CS3-FLAG-EEVD), which has the tetrapeptide motif at the carboxyl terminus. CS3-FLAG-EEVD, but not CS-FLAG, efficiently bound to His-Tom60ΔN-HA (Fig. 4c). These results indicate that the EhTom60 is involved in the mitosomal transport of membrane proteins via cytosolic Hsp70 and Hsp90.

Discussion

We have demonstrated that *Entamoeba* possesses Tom60, a novel genus-specific peripheral membrane component of the TOM complex, that functions as a receptor/carrier to transport mitosomal proteins from the cytoplasm to mitosomes. One of the striking features of Tom60 is its bipartite localization, which allows Tom60 to function as a carrier of *de novo* synthesized mitosomal preproteins in the cytoplasm and a structural component of the TOM complex on the mitosomal membrane. In this respect, *Entamoeba* Tom60 resembles a mammalian peripheral membrane protein, Tom34, which serves as a co-chaperone of Hsp70 and Hsp90 in a Tom70-dependent transport[33]. However, there is a clear difference between *Entamoeba* Tom60 and mammalian Tom34. Tom60 has direct physical interaction with TOM complex, whereas Tom34 is indirectly associated with Tom40 via Tom22 and Tom70[33,34]. Moreover, *Entamoeba* Tom60 appears to play an indispensable role, judged from the severe growth defect caused by gene silencing (knock down), similar to yeast Tom20 and Tom70[35], whereas Tom34-deficient mice were

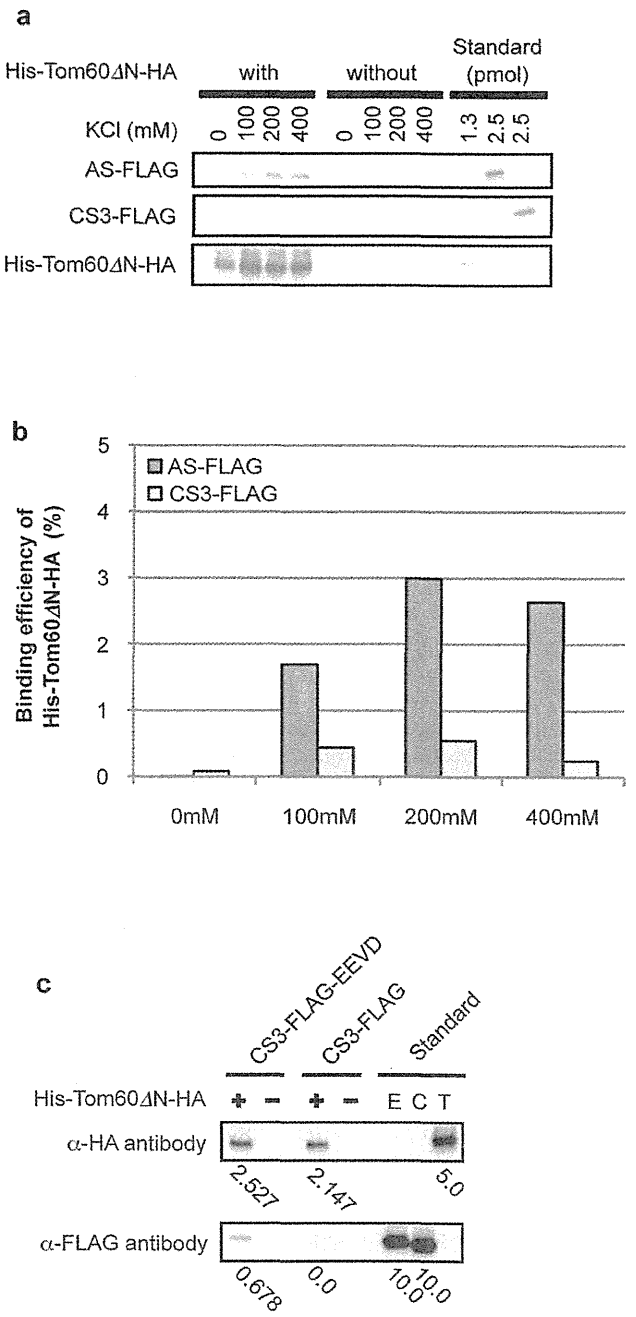

Figure 4 | *In vitro* binding assay of Tom60 and a mitosomal protein. (a), Immunoblotting of proteins bound to His-Tom60ΔN-HA. AS-FLAG is a mitosomal matrix protein, while CS3-FLAG is a cytosolic protein as a control. Approximately 40% of the whole eluates and 1.3 or 2.5% of standards used for the binding assay were subjected to SDS-PAGE and immunoblot analyses with anti-HA and anti-FLAG mouse monoclonal antibody (clone M2, Sigma-Aldrich Japan). (b), Relative binding efficiency of His-Tom60ΔN-HA towards a mitosomal matrix protein. The data were quantitated based on the result shown in Fig. 4a. Vertical and horizontal axes indicate the binding efficiency of His-Tom60ΔN-HA towards substrates and the KCl concentrations, respectively. Low bars in the graph are described numerically while measurements and calculations are described in Supplementary Fig. S7 and Supplementary Methods. (c), The verification of interaction between His-Tom60ΔN-HA and the "EEVD" motif. CS3-FLAG-EEVD is an engineered cytosolic protein in which the "EEVD" motif was added to the carboxyl terminus, like in cytosolic Hsp70 and Hsp90, while CS3-FLAG is a negative control. Approximately 50% of the whole eluates and 5.0 or 10.0 pmol of standards used for the binding assay were subjected to SDS-PAGE and immunoblot analysis, as described above. "E", "C", and "T" stand for CS3-FLAG-EEVD, CS3-FLAG, and His-Tom60ΔN-HA, respectively. Values below panels indicate protein amounts (pmol) estimated by densitometric scanning of the blots.

viable, grew normally, and had a normal Mendelian inheritance pattern[36]. Thus, *Entamoeba* Tom60 represents an unprecedented essential bipartite-localized receptor/carrier for the protein import to MROs. It was presumed that Tom20 and Tom70 are loosely associated with other components of TOM complex, mobilized on the entire mitochondrial surface, and capable of interacting with preproteins[37]. Similarly, we assume that cytosolic localization of the *Entamoeba* Tom60 also maximizes the chance of its interaction with mitosomal preproteins. The mechanisms of the recruitment of Tom60 to the mitosomal outer membrane remain unsolved. One possibility is that Tom60 loaded with a precursor protein docks to the TOM complex, whereas free unloaded Tom60 remains dissociated from the TOM complex in the cytosol. Another possibility is the post-translational modifications. It has been recently reported that the binding of mammalian Tom20 and Tom70 toward preproteins is regulated by phosphorylation[38].

Tom60 is a robust receptor for the mitosomal transport. Tom60 seems to transport both soluble and membrane mitosomal proteins. It has been shown in Opisthokonta that mitochondrial soluble matrix and membrane preproteins are transported via binding with distinct TPR-containing mitochondrial receptors, namely Tom20 and Tom70, which recognizes the amino-terminal transit peptide or the internal (cryptic) targeting signals, respectively[31]. Subsequently, these preproteins are passed from Tom20 and Tom70 to Tom22 and inserted into the Tom40 channel[31]. Therefore, Tom22 plays a role as a receptor for both mitochondrial soluble matrix and membrane preproteins. Similarly, *Entamoeba* Tom60 binds to a soluble mitosomal matrix protein, AS, as well as the "EEVD" motif, which is conserved in cytosolic Hsp70 and Hsp90 from three *Entamoeba* species. It was demonstrated that in mammals, cytosolic Hsp70 and Hsp90 are involved in the Tom70-dependent transport of mitochondrial membrane preproteins to TOM complex[39]. Among MRO-containing eukaryotes, no organism that possesses both Tom70 and Tom20 has been discovered. *Encephalitozoon*[1] and *Blastocystis*[40,41] encodes only a Tom70 homolog, suggesting that the Tom70 homolog may play a bifunctional role similar to *Entamoeba* Tom60. In contrast, in *Giardia*[42], *Trichomonas*[43], and *Cryptosporidium*[44], no potential receptor component of TOM complex has been identified. These organisms most likely possess a lineage-specific receptor like *Entamoeba* Tom60. Further investigation is needed to clarify if such lineage-specific functional Tom60 homologs also contain the TPR domains for the cargo interaction.

It was hypothesized that the TOM complex in early eukaryotes is composed of Tom40, Tom22, and Tom7[17]. It was also shown that the TOM complex of the aerobic free-living social amoebozoan *D. discoideum* consists of Tom40, Tom22, Tom7, and Tom6, and lacks Tom20 and Tom70[7,13]. These data indicate that a common ancestor of amoebozoan species also contained Tom40, Tom22, and Tom7 in its TOM complex. This presumption is also supported by the existence of Tom40 homologs in the genome of other amoebozoan species including *Polysphondylium*[45], and *Acanthamoeba*[45], and the transcriptome of *Mastigamoeba* (Stairs, C. and Roger, A., personal communication), and Tom7 homologs in *Polysphondylium* (EFA78398) and *Acanthamoeba* (Contig6955 in the *Acanthamoeba* genome database). However, we did not detect Tom22 homologs in these amoebozoa. These data are consistent with the premise that *Entamoeba* probably secondarily has lost Tom22 during separation within Amoebozoa. A key question regarding a lineage-specific presence of Tom60 in *Entamoeba* is why and how the loss of the

canonical subunit Tom22 and gain of Tom60 occurred. We presume that it is related to the lack of mitosomal targeting sequences in *Entamoeba*[9]. In the general model of mitochondrial matrix protein import, Tom22 interacts with the positive-charged surface in the amphiphilic α-helix of presequences[30,46]. In contrast, such ionic interaction does not appear to mediate the binding between *Entamoeba* Tom60 and mitosomal proteins. An alternative explanation of the loss of Tom22 is that in the *Entamoeba* ancestor the mitosomal proteins that were acquired by lateral gene transfer, such as sulfate activation enzymes, were poorly imported into mitosomes by Tom22.

Our current hypothesis as to how a novel TOM complex evolved in *Entamoeba* mitosomes is as follows: The *Entamoeba* ancestor was exposed to anaerobic environments, under which oxygen-dependent energy generation became unusable. Under these conditions, the mitochondrion lost its electron transport chain, membrane potential, and other aerobic mitochondrion-related functions. The loss of membrane potential across the inner membrane promoted an elimination of the canonical membrane potential-dependent TIM23 and TIM22 complexes[31]. In agreement with this hypothesis, membrane potential-dependent AAC, that is present in the aerobic mitochondria, became non-reliant on the membrane potential in *E. histolytica*[23]. Moreover, as described above, *Entamoeba* mitosomal proteins lack a canonical positively-charged transit peptide[9], which is utilized for the electrophoretic import via the membrane potential[31]. Alterations of the TIM complex led to the rearrangement of the TOM complex, more specifically loss of Tom22, which is associated with the TIM23 complex in a typical aerobic mitochondrion. Finally, loss of Tom22 must have been compensated with the invention of a new targeting mechanism dependent on Tom60. It was also suggested that subunit replacement might have occurred in the TIM complex of *Trichomonas vaginalis*[43] and *Giardia intestinalis*[42]. It is worth further investigating how commonly replacement of subunits occurred in anaerobic MRO-possessing eukaryotes.

Methods

Organisms. Trophozoites of *Entamoeba histolytica* HM-1:IMSS cl6[47] and G3[48] strains were cultivated axenically in Diamond BI-S-33 medium[49].

RNA and cDNA preparation. Total RNA was isolated from various strains by TRIZOL® reagent (Invitrogen, Carlsbad, San Diego, CA). mRNA was purified using GenElute™ mRNA Miniprep Kits (Sigma-Aldrich Japan). cDNA was synthesized from mRNA using SuperScript™ III RNase H⁻ reverse transcriptase (Invitrogen), oligo(dT)$_{20}$ primer, and primer 1 (Supplementary Table S5).

Plasmid construction. *E. histolytica Tom40* and *Tom60* genes were PCR-amplified from cDNA using Phusion DNA polymerase (New England Biolabs, Beverly, MA) and corresponding primer sets (Supplementary Table S5). After restriction digestion, amplified fragments were ligated into pEhEx/HA[50] and pEhEx/Myc[29] using Ligation-Convenience Kit (Nippongene, Tokyo, Japan). To generate the plasmid for Tom40-Myc/Tom60-HA double-expression, a fragment containing the Tom40-Myc protein coding region flanked by the upstream and downstream regions of the *CS1* gene was PCR-amplified from pEhEx/Tom40-Myc by primers 6/7 (Supplementary Table S5), and inserted into the *Spe* I-digested pEhEx/Tom60-HA using In-Fusion® system (TaKaRa, Shiga, Japan). For gene silencing, a 400-bp fragment corresponding to the amino terminus of Tom40 and Tom60 was PCR-amplified with appropriate primers (Supplementary Table S5). Restriction-digested fragments were ligated into *Stu* I/*Sac* I double-digested psAP-2-Gunma plasmid[27].

Amoeba transformation. Lipofection of trophozoites, selection, and maintenance of transformants were performed as previously described[9].

Immunofluorescence assay. IFA[9,51] was performed as previously described.

Preparation of organelle fraction. Amoeba strains that expressed HA-tagged Tom60-HA, Tom40-HA, AAC-HA, APSK-HA, and CPBF1-HA[29] proteins, strains in which *Tom40* and *Tom60* genes were silenced, and mock transformants (pEhEx/HA and psAP2-Gunma) were washed three times with 2% glucose/PBS. After resuspension in lysis buffer (10 mM MOPS-KOH, pH7.2, 250 mM sucrose, protease inhibitors), cells were disrupted mechanically by a Dounce homogenizer. Unbroken cells were removed by centrifugation at 5,000 × *g* for 10 min, and the supernatant centrifuged at 100,000 × *g* for 60 min to separate the organelle and cytosolic fractions. The 100,000 × *g* organelle fractions were resuspended with lysis buffer, and were recollected by the centrifugation at 100,000 × *g* for 60 min.

Immunoprecipitation of the TOM complex. Organelle fractions were solubilized with IP buffer (2% digitonin/50 mM BisTris-HCl, pH7.2/50 mM NaCl/10% [W/V] glycerol, protease inhibitors). The lysate was mixed with Protein G-Sepharose 4 Fast Flow (GE Healthcare), and Sepharose beads were removed by centrifugation. Precleared lysates were mixed with anti-HA mouse monoclonal antibody conjugated with agarose (Sigma-Aldrich Japan) at 4°C for 3 h. Agarose was washed three times with IP buffer containing 1% digitonin. Bound protein was eluted by IP buffer containing 1% digitonin and 600 μg/ml HA peptide (Sigma-Aldrich Japan).

Blue native polyacrylamide gel electrophoresis (BN-PAGE). Organelle fractions were solubilized by either 2% digitonin or n-dodecyl-β-D-maltoside (DDM) at 4°C for 30 min, and centrifuged at 20,000 × *g* for 30 min at 4°C. BN-PAGE was performed using NativePAGE™ Novex® Bis-Tris Gel System (Invitrogen) according to manufacturer's protocol. Immunoprecipitated samples were mixed with 0.25% Coomassie® G-250 (Invitrogen) before electrophoresis.

Liquid chromatography-tandem mass spectrometric analysis. In-gel trypsin digestion of protein bands of interest and LC-MS/MS were performed as previously described[52,53].

Proteinase K treatment. Organelle fractions (50 μg protein each) were treated with or without final 2.8 μg/ml proteinase K (Roche) at 4°C for 15 min, followed by SDS-PAGE and immunoblot analysis with anti-HA mouse monoclonal antibody. Band intensities were evaluated using the Analysis Toolbox in ImageQuant TL software (GE Healthcare).

Na_2CO_3 treatment. Organelle fractions (1 mg protein) in lysis buffer were diluted 20 times with ice-cold 100 mM Na_2CO_3, pH 11.5 and 150 mM NaCl, kept at 4°C for 30 min, and centrifuged at 100,000 × *g* for 60 min. The 100,000 × *g* supernatant was transferred to a fresh tube and the precipitate washed once with Na_2CO_3 solution. Immunoblot analysis was performed as described above. Anti-PNT (1 : 1,000) and anti-APSK (1 : 1,000) rabbit antisera were used as primary antibodies. Alkaline phosphatase-conjugated anti-rabbit IgG antibody (Jackson ImmunoResearch, West Grove, PA) was used as secondary antibody.

Quantitative real-time PCR. Quantitative real-time PCR analysis was performed as described[27] using primer sets (primers 12-25; Supplementary Table S5) for *Tom40*, *Tom60*, *Cpn60*, *AS*, *APSK*, *IPP*, and *Rnapol* (XM_643999) genes.

Recombinant proteins. To generate recombinant histidine tagged (His_6)-Tom60ΔN-HA, AS-FLAG, CS3-FLAG, and CS3-FLAG-EEVD proteins, we amplified *Tom60*, *AS*, and *CS3* genes using appropriate primers sets (Supplementary Table S5) and pEhEx/Tom60-HA, pEhEx/AS-HA[9], and pET15b/CS3[54] as templates. Fragments were digested by appropriate sets of restriction enzymes and ligated into pCold I (TaKaRa). These plasmids were transformed into BL21 Star™(DE3) One Shot® Chemically Competent *E. coli* (Invitrogen) and expression of recombinant proteins was induced by 1 mM IPTG. After lysis of bacteria and purification by Ni-NTA system (QIAGEN GmbH, Hilden, Germany), the His_6-tag was removed from His_6-AS-FLAG, His_6-CS-FLAG and His_6-CS-FLAG-EEVD by AcTEV™ protease (Invitrogen).

***In vitro* binding assay of Tom60.** The binding efficiency of His_6-Tom60ΔN-HA was calculated and shown as the ratio of eluted AS-FLAG or CS3-FLAG to that of eluted His-Tom60ΔN-HA in the *in vitro* binding assay (Supplementary Methods). The hydrophobic nature of the amino terminus of Tom60 negatively affected solubility, thus it was removed prior to the binding assay. To verify the interaction between His_6-Tom60ΔN-HA and the "EEVD" motif, we carried out the assay with CS3-FLAG-EEVD or CS3-FLAG. Assay condition was identical to *in vitro* binding assay as described in Supplementary Methods except that the assay buffer contained 50 mM KCl.

1. Lill, R. & Kispal, G. Maturation of cellular Fe-S proteins: an essential function of mitochondria. *Trends Biochem Sci.* **8**, 352–356 (2000).
2. Maralikova, B. *et al.* Bacterial-type oxygen detoxification and iron-sulfur cluster assembly in amoebal relict mitochondria. *Cell Microbiol.* **3**, 331–342 (2010).
3. Tovar, J. *et al.* Mitochondrial remnant organelles of *Giardia* function in iron-sulphur protein maturation. *Nature.* **426**, 172–176 (2003).
4. Sutak, R. *et al.* Mitochondrial-type assembly of FeS centers in the hydrogenosomes of the amitochondriate eukaryote *Trichomonas vaginalis*. *Proc Natl Acad Sci U S A.* **101**, 10368–10373 (2004).
5. Goldberg, A. V. *et al.* Localization and functionality of microsporidian iron-sulphur cluster assembly proteins. *Nature.* **452**, 624–628 (2008).
6. Tsaousis, A. D. *et al.* Evolution of Fe/S cluster biogenesis in the anaerobic parasite *Blastocystis*. *Proc Natl Acad Sci U S A.* **109**, 10426–10431 (2012).
7. Lithgow, T. & Schneider, A. Evolution of macromolecular import pathways in mitochondria, hydrogenosomes and mitosomes. *Philos Trans R Soc Lond B Biol Sci.* **365**, 799–817 (2010).
8. Heinz, E. & Lithgow, T. Back to basics: A revealing secondary reduction of the mitochondrial protein import pathway in diverse intracellular parasites. *Biochim Biophys Acta.* In press (2012).

9. Mi-ichi, F., Yousuf, M. A., Nakada-Tsukui, K. & Nozaki, T. Mitosomes in *Entamoeba histolytica* contain a sulfate activation pathway. *Proc Natl Acad Sci USA.* **106**, 21731–21736 (2009).
10. Dagley, M. J. *et al.* The protein import channel in the outer mitosomal membrane of *Giardia intestinalis*. *Mol Biol Evol.* **9**, 1941–1947 (2009).
11. Dyall, S. D. *et al. Trichomonas vaginalis* Hmp35, a putative pore-forming hydrogenosomal membrane protein, can form a complex in yeast mitochondria. *J Biol Chem* **278**, 30548–30561 (2003).
12. Shiflett, A. M. & Johnson, P. J. Mitochondrion-related organelles in eukaryotic protists. *Annu Rev Microbiol.* **64**, 409–429 (2010).
13. Dolezal, P. *et al.* The essentials of protein import in the degenerate mitochondrion of *Entamoeba histolytica*. *PLoS Pathog.* **6**, e1000812 (2010).
14. Dolezal, P., Likic, V., Tachezy, J. & Lithgow, T. Evolution of the molecular machines for protein import into mitochondria. *Science.* **313**, 314–318 (2006).
15. Hoogenraad, N. J., Ward, L. A. & Ryan, M. T. Import and assembly of proteins into mitochondria of mammalian cells. *Biochim Biophys Acta.* **1592**, 97–105 (2002).
16. Pfanner, N., Wiedemann, N., Meisinger, C. & Lithgow, T. Assembling the mitochondrial outer membrane. *Nat Struct Mol Biol.* **11**, 1044–1048 (2004).
17. Maćasev, D. *et al.* Tom22', an 8-kDa trans-site receptor in plants and protozoans, is a conserved feature of the TOM complex that appeared early in the evolution of eukaryotes. *Mol Biol Evol.* **8**, 1557–1564 (2004).
18. Chew, O. *et al.* A plant outer mitochondrial membrane protein with high amino acid sequence identity to a chloroplast protein import receptor. *FEBS Lett.* **557**, 109–114 (2004).
19. Pusnik, M. *et al.* Mitochondrial preprotein translocase of trypanosomatids has a bacterial origin. *Curr Biol.* **21**, 1738–1743 (2011).
20. Perry, A. J., Hulett, J. M., Likić, V. A., Lithgow, T. & Gooley, P. R. Convergent evolution of receptors for protein import into mitochondria. *Curr Biol.* **16**, 221–229 (2006).
21. Stanley, S. L. Jr. Amoebiasis. *Lancet.* **361**, 1025–1034 (2003).
22. León-Avila, G. & Tovar, J. Mitosomes of *Entamoeba histolytica* are abundant mitochondrion-related remnant organelles that lack a detectable organellar genome. *Microbiology.* **150**, 1245–1250 (2004).
23. Chan, K. W. *et al.* A novel ADP/ATP transporter in the mitosome of the microaerophilic human parasite *Entamoeba histolytica*. *Curr Biol.* **15**, 737–742 (2005).
24. Model, K. *et al.* Multistep assembly of the protein import channel of the mitochondrial outer membrane. *Nat Struct Biol.* **8**, 361–370 (2001).
25. Karpenahalli, M. R., Lupas, A. N. & Söding, J. TPRpred: a tool for prediction of TPR-, PPR- and SEL1-like repeats from protein sequences. *BMC Bioinformatics.* **8**, 2. (2007).
26. Baker, M. J., Frazier, A. E., Gulbis, J. M. & Ryan, M. T. Mitochondrial protein-import machinery: correlating structure with function. *Trends Cell Biol.* **17**, 456–464 (2007).
27. Mi-ichi, F. *et al.* Sulfate activation in mitosomes plays an important role in the proliferation of *Entamoeba histolytica*. *PLoS Negl Trop Dis.* **5**, e1263 (2011).
28. Fujiki, Y. *et al.* Polypeptide and phospholipid composition of the membrane of rat liver peroxisomes: comparison with endoplasmic reticulum and mitochondrial membranes. *J Cell Biol.* **93**, 103–110 (1982).
29. Nakada-Tsukui, K. *et al.* A novel class of cysteine protease receptors that mediate lysosomal transport. *Cell Microbiol.* **14**, 1299–1317 (2012).
30. Brix, J., Dietmeier, K. & Pfanner, N. Differential recognition of preproteins by the purified cytosolic domains of the mitochondrial import receptors Tom20, Tom22, and Tom70. *J. Biol. Chem.* **272**, 20730–20735 (1997).
31. Chacinska, A. *et al.* Importing mitochondrial proteins: machineries and mechanisms. *Cell.* **138**, 628–644 (2009).
32. Young, J. C., Hoogenraad, N. J. & Hartl, F. U. Molecular chaperones Hsp90 and Hsp70 deliver preproteins to the mitochondrial import receptor Tom70. *Cell.* **112**, 41–50 (2003).
33. Faou, P. & Hoogenraad, N. J. Tom34: a cytosolic cochaperone of the Hsp90/Hsp70 protein complex involved in mitochondrial protein import. *Biochim Biophys Acta.* **1823**, 348–357 (2012).
34. van Wilpe, S. *et al.* Tom22 is a multifunctional organizer of the mitochondrial preprotein translocase. *Nature.* **401**, 485–489 (1999).
35. Moczko, M. *et al.* Deletion of the receptor MOM19 strongly impairs import of cleavable preproteins into *Saccharomyces cerevisiae* mitochondria. *J Biol Chem.* **269**, 9045–9051 (1994).
36. Terada, K. *et al.* Expression of Tom34 splicing isoforms in mouse testis and knockout of Tom34 in mice. *J Biochem.* **133**, 625–631 (2003).
37. Dekker, P. J. *et al.* Preprotein translocase of the outer mitochondrial membrane: Molecular dissection and assembly of the general import pore complex. *Mol Cell Biol.* **18**, 6515–6524 (1998).
38. Schmidt, O. *et al.* Regulation of mitochondrial protein import by cytosolic kinases. *Cell.* **144**, 227–239 (2011).
39. Young, J. C., Hoogenraad, N. J. & Hartl, F. U. Molecular chaperones Hsp90 and Hsp70 deliver preproteins to the mitochondrial import receptor Tom70. *Cell.* **112**, 41–50 (2003).
40. Denoeud, F. *et al.* Genome sequence of the stramenopile *Blastocystis*, a human anaerobic parasite. *Genome Biol.* **12**, R29 (2011).
41. Tsaousis, A. D. *et al.* A functional Tom70 in the human parasite *Blastocystis* sp.: implications for the evolution of the mitochondrial import apparatus. *Mol Biol Evol.* **28**, 781–791 (2011).
42. Jedelský, P. L. *et al.* The minimal proteome in the reduced mitochondrion of the parasitic protist *Giardia intestinalis*. *PLoS One.* **6**, e17285 (2011).
43. Rada, P. *et al.* The core components of organelle biogenesis and membrane transport in the hydrogenosomes of *Trichomonas vaginalis*. *PLoS One.* **6**, e24428 (2011).
44. Alcock, F. *et al.* A small Tim homohexamer in the relict mitochondrion of *Cryptosporidium*. *Mol Biol Evol.* **29**, 113–122 (2012).
45. Wojtkowska, M. *et al.* Phylogenetic analysis of mitochondrial outer membrane β-barrel channels. *Genome Biol Evol.* **4**, 110–125 (2012).
46. Yamano, K. *et al.* Tom20 and Tom22 share the common signal recognition pathway in mitochondrial protein import. *J Biol Chem.* **283**, 3799–3807 (2008).
47. Diamond, L. S., Mattern, C. F. & Bartgis, I. L. Viruses of *Entamoeba histolytica*. I. Identification of transmissible virus-like agents. *J Virol.* **9**, 326–341 (1972).
48. Bracha, R., Nuchamowitz, Y., Anbar, M. & Mirelman, D. Transcriptional silencing of multiple genes in trophozoites of *Entamoeba histolytica*. *PLoS Pathog.* **2**, e48 (2006).
49. Diamond, L. S., Harlow, D. R. & Cunnick, C. C. A new medium for the axenic cultivation of *Entamoeba histolytica* and other. *Entamoeba. Trans R Soc Trop Med Hyg* **72**, 431–432 (1978).
50. Nakada-Tsukui, K., Okada, H., Mitra, B. N. & Nozaki, T. Phosphatidylinositol-phosphates mediate cytoskeletal reorganization during phagocytosis via a unique modular protein consisting of RhoGEF/DH and FYVE domains in the parasitic protozoon *Entamoeba histolytica*. *Cell Microbiol.* **11**, 1471–1491 (2009).
51. Nakada-Tsukui, K., Saito-Nakano, Y., Ali, V. & Nozaki, T. A Retromerlike Complex Is a Novel Rab7 Effector That Is Involved in the Transport of the Virulence Factor Cysteine Protease in the Enteric Protozoan Parasite *Entamoeba histolytica*. *Mol Biol Cell.* **16**, 5294–5303 (2005).
52. Mineki, R. *et al. In situ* alkylation with acrylamide for identification of cysteinyl residues in proteins during one- and two-dimensional sodium dodecyl sulphate-polyacrylamide gel electrophoresis. *Proteomics.* **2**, 1672–1681 (2002).
53. Makiuchi, T. *et al.* Compartmentalization of a glycolytic enzyme in Diplonema, a non-kinetoplastid euglenozoan. *Protist.* **162**, 482–489 (2011).
54. Husain, A. *et al.* Metabolome Analysis Revealed Increase in *S*-Methylcysteine and Phosphatidylisopropanolamine Synthesis upon l-Cysteine Deprivation in the Anaerobic Protozoan Parasite *Entamoeba histolytica*. *J Biol Chem.* **285**, 39160–39170 (2010).
55. Yousuf, M. A., Mi-ichi, F., Nakada-Tsukui, K. & Nozaki, T. Localization and targeting of an unusual pyridine nucleotide transhydrogenase in *Entamoeba histolytica*. *Eukaryot Cell.* **9**, 926–933 (2010).

Acknowledgments

We thank Tsutomu Fujimura, Reiko Mineki, and Hikari Taka, the Division of Proteomics and Biomolecular Science, Biomedical Research Center at Juntendo University Graduate School of Medicine for mass-spectrometric analysis, Courtney Spears and Andrew J. Roger, Centre for Comparative Genomics and Evolutionary Bioinformatics, Department of Biochemistry and Molecular Biology at Dalhousie University for the information on *Mastigamoeba* transcriptome, Ghulam Jeelani and Eiko Nakasone for technical assistance, and Gil M. Penuliar and Herbert Santos for proof reading. This work was supported by a Grant-in-Aid for Scientific Research from the Ministry of Education, Culture, Sports, Science and Technology (MEXT) of Japan to T.N. (23117001, 23117005, 23390099), a Grant-in-Aid on Bilateral Programs of Joint Research Projects and Seminars from Japan Society for the Promotion of Science, a Grant-in-Aid on Strategic International Research Cooperative Program from Japan Science and Technology Agency, a grant for research on emerging and re-emerging infectious diseases from the Ministry of Health, Labour and Welfare of Japan (H23-Shinko-ippan-014) to T.N., a grant for research to promote the development of anti-AIDS pharmaceuticals from the Japan Health Sciences Foundation (KHA1101) to T.N., Strategic International Research Cooperative Program from Japan Science and Technology Agency to T.N. and by Global COE Program (Global COE for Human Metabolomic Systems Biology) from MEXT, Japan to T.N.

Author contributions

T.M. did the experiments. T.M. and T.N. wrote the manuscript. T.M., F.M., K.N.-T. and T.N. interpreted the data.

Additional information

Supplementary information accompanies this paper at http://www.nature.com/scientificreports

Competing financial interests: The authors declare no competing financial interests.

How to cite this article: Makiuchi, T., Mi-ichi, F., Nakada-Tsukui, K. & Nozaki, T. Novel TPR-containing subunit of TOM complex functions as cytosolic receptor for *Entamoeba* mitosomal transport. *Sci. Rep.* 3, 1129; DOI:10.1038/srep01129 (2013).

IAI
Journals.ASM.org

Cysteine Protease-Binding Protein Family 6 Mediates the Trafficking of Amylases to Phagosomes in the Enteric Protozoan *Entamoeba histolytica*

Atsushi Furukawa,[a,b]* Kumiko Nakada-Tsukui,[a] Tomoyoshi Nozaki[a,c]

Department of Parasitology, National Institute of Infectious Diseases, Toyama, Tokyo, Japan[a]; Department of Parasitology, Gunma University Graduate School of Medicine, Maebashi, Japan[b]; Graduate School of Life and Environmental Sciences, University of Tsukuba, Tsukuba, Ibaraki, Japan[c]

Phagocytosis plays a pivotal role in nutrient acquisition and evasion from the host defense systems in *Entamoeba histolytica*, the intestinal protozoan parasite that causes amoebiasis. We previously reported that *E. histolytica* possesses a unique class of a hydrolase receptor family, designated the cysteine protease-binding protein family (CPBF), that is involved in trafficking of hydrolases to lysosomes and phagosomes, and we have also reported that CPBF1 and CPBF8 bind to cysteine proteases or β-hexosaminidase α-subunit and lysozymes, respectively. In this study, we showed by immunoprecipitation that CPBF6, one of the most highly expressed CPBF proteins, specifically binds to α-amylase and γ-amylase. We also found that CPBF6 is localized in lysosomes, based on immunofluorescence imaging. Immunoblot and proteome analyses of the isolated phagosomes showed that CPBF6 mediates transport of amylases to phagosomes. We also demonstrated that the carboxyl-terminal cytosolic region of CPBF6 is engaged in the regulation of the trafficking of CPBF6 to phagosomes. Our proteome analysis of phagosomes also revealed new potential phagosomal proteins.

Phagocytosis and phagosome biogenesis play indispensable and pivotal roles in the pathogenesis of *Entamoeba histolytica*. *E. histolytica* trophozoites ingest and digest microorganisms in the large intestine, for the acquisition of nutrients (1), and also host cells (2) during tissue invasion, for the creation of a parasitic niche. Phagocytosis also plays a role in the evasion from host immune systems (3). It has been demonstrated that the levels of *in vitro* and *in vivo* virulence of clinical and laboratory strains correlate well with the ability for phagocytosis (4–7). In addition, phagosomes contain a panel of proteins that have been implicated in pathogenesis, such as cysteine proteases (CPs) (8), amoeba pores (9), and galactose-/*N*-acetylgalactosamine-specific lectin (10, 11). Therefore, an understanding of the molecular mechanisms of phagosome biogenesis and trafficking, together with the characterization of "uncharacterized hypothetical" proteins in phagosomes, should further uncover the links between phagocytosis and pathogenicity.

Recently, the molecular mechanisms of phagocytosis have started to be unveiled. For example, an unconventional myosin, myosin IB, was shown to be involved in cytoskeleton rearrangement during phagocytosis (12). It was also shown that phosphatidylinositol signaling is involved in phagocytosis. The time- and position-specific accumulations of phosphatidylinositol-3-phosphate (PI3P) and phosphatidylinositol (3,4,5)-trisphosphate (PIP3) (13–15) on the phagosomal membrane were demonstrated. Surface Ca^{2+}-binding kinase (C2PK) was shown to be involved in the initiation of phagocytosis (16). C2PK localizes in close proximity to the plasma membrane through phosphatidylserine in the presence of Ca^{2+} and thereby recruits *E. histolytica* CaBP1 (EhCaBP1) and actin to the phagocytic cup during erythrophagocytosis. Conditional suppression of C2PK expression and overexpression of a mutant form demonstrated its role in the initiation of the formation of the phagocytic cup. Surface transmembrane kinase (TMK96) and p21-activated kinase (PAK) also have been shown to play important roles in phagocytosis of human erythrocytes (17, 18). TMK96 was identified in the proteome of isolated phagosomes and plays an important role in the clearance of dead host cells. PAK was shown to be highly concentrated in the nascent pseudopod in motile trophozoites and appears to be a regulatory element controlling pseudopod extension and cell polarity. Overproduction of the carboxyl-terminal kinase domain of PAK causes multiple pseudopod formation and enhanced erythrophagocytosis.

Although the mechanisms of initiation of phagocytosis have been vigorously investigated, it is only recently that scientists have started to understand the fundamental mechanisms of how hydrolases are selectively transported to phagosomes, leading to organelle maturation. Transport and activation of hydrolytic enzymes are tightly regulated. Otherwise, they are deleterious to the cell. In yeast and mammals, trafficking of major hydrolytic enzymes is mediated by the specific cargo receptors mannose-6-phosphate receptor (M6PR) and Vps10/sortilin. M6PR regulates the trafficking of M6P-modified lysosomal hydrolases, including cathepsin L and β-hexosaminidase, while Vps10p/sortilin regulates the trafficking of carboxypeptidase Y in yeast or cathepsin D in mammals. *E. histolytica* appears to lack a Vps10/sortilin ho-

Received 30 August 2012 Returned for modification 4 October 2012
Accepted 10 December 2012
Published ahead of print 18 March 2013
Editor: J. F. Urban, Jr.
Address correspondence to Tomoyoshi Nozaki, nozaki@nih.go.jp.
* Present address: Atsushi Furukawa, Laboratory of Bimolecular Science, Faculty of Pharmaceutical Sciences, Hokkaido University, Japan.
Supplemental material for this article may be found at http://dx.doi.org/10.1128/IAI.00915-12.

doi:10.1128/IAI.00915-12